Frank-Kasper phases in block polymers

Kevin D. Dorfman*

Department of Chemical Engineering and Materials Science, University of Minnesota, Twin–Cities, 421 Washington Ave SE, Minneapolis, MN 55455, USA

E-mail: dorfman@umn.edu

Abstract

The discovery of the Frank-Kasper σ phase in diblock copolymer and tetrablock terpolymer melts catalyzed a renewed interest over the past decade in understanding particle-forming phases in block polymer systems. This Perspectives article provides a concise overview of the Frank-Kasper phases seen to date in block polymers (A15, σ, and the C14 and C15 Laves phases) and mechanisms known to produce them: conformational asymmetry in neat diblock copolymer melts; interfacial segregation effects in diblock copolymer blends; particle swelling in diblock copolymer/homopolymer blends; and matrix segregation effects in neat tetrablock terpolymer melts. While a qualitative understanding of the emergence of Frank-Kasper phases in block polymer systems has been achieved, a number of outstanding questions remain, in particular those arising from the low degree of polymerization used in experiments, non-equilibrium effects during thermal processing, and the large design space available in blends and multiblock systems. This Perspective discusses potential avenues for future research related to these areas, as well as overarching issues underlying the connections between Frank-Kasper phase formation in block polymers to other soft matter and metals.

*To whom correspondence should be addressed

Introduction

When a block polymer melt is cooled below its order-disorder transition, it adopts an ordered structure that balances the entropic cost of chain stretching against the enthalpic penalty of interfacial tension, subject to the constraint of filling space at a uniform density. Like many thermodynamic principles, this seemingly simple statement has profound implications. We are interested here in the manifestation of this principle primarily for compositionally asymmetric diblock copolymers, where the volume fraction of the minority block is small. In this case, the optimal balance of chain stretching and interfacial tension is realized by forming micellar particles, illustrated in Fig. 1, with the minority block in the particle core. Similar packing is realized as well in (i) "pseudo-diblock" multiblock polymers,[1] where one block with a small volume fraction is segregated from the other blocks, which themselves exhibit at most weak segregation in the matrix, and (ii) blends of diblock polymers[2] or diblock polymer/homopolymer blends[3] with appropriate compositions to promote spherical micelle formation. While the particles formed in such systems would adopt a spherical micelle conformation in dilute solution, spherical particles cannot fill space in a melt without leaving gaps. As a result, below the order-disorder transition the micelles adopt a polyhedral shape that reflects the Wigner-Seitz cells of the underlying lattice (Fig. 1).

The selection of the ordered state can be posed as identifying the least expensive distortion of the otherwise spherical particle to fill space.[5] For decades, there was a general consensus that the optimal particle packing for diblock copolymers is the body-centered cubic (bcc) lattice in Fig. 1,[6,7] with self-consistent field theory (SCFT) predicting a very narrow region of close packed spheres (face-centered cubic, fcc, or hexagonally close-packed, hcp) near the order-disorder transition.[8,9] Theory predicts that the close-packed structure predicted in the mean-field limit is destroyed by fluctuations at finite molecular weights,[10] although close packing has been observed experimentally.[11–13] The consensus surrounding the formation of a bcc lattice, achieved in the 1980s,[14,15] was upended by the theoretical prediction of a Frank-Kasper A15 phase in a multiply branched block polymer by Grason and coworkers in

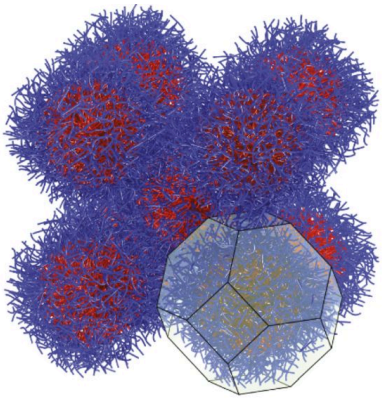

Figure 1: Illustration of the packing of compositionally asymmetric diblock polymer melt into particles where the minority block forms the particle cores. Owing to the need to fill space, the particles are polyhedral. The packing illustrated here is bcc, where the particles have eight nearest neighbors. Adapted with permission from Reddy, A.; Buckley, M. B.; Arora, A.; Bates, F. S.; Dorfman, K. D.; Grason, G. M. Stable Frank-Kasper phases of self-assembled, soft matter spheres. *Proc. Natl. Acad. Sci. USA* **2018**, *115*, 10233–10238. Copyright 2018 by the authors.

2003[16] and the subsequent discovery of a Frank-Kasper σ phase in both a diblock copolymer and a tetrablock terpolymer by Bates and coworkers in 2010.[17]

These discoveries have sparked a renewed interest in examining the particle-forming region of the diblock phase diagram and related particle-forming phases in multiblock polymers and block polymer blends. There are three driving factors behind this interest, two fundamental and one practical. The first factor is simply the recognition that what appeared to be a well understood problem is anything but well understood, exposing an unexplored and fertile area for materials discovery. What drives the formation of Frank-Kasper phases in block polymers? There are a vast number of packings that satisfy the rules for forming a Frank-Kasper phase;[18] how many of these phases exist in block polymers? These questions, amongst others, form the main focus of this Perspective. The second factor is potential connections between particle-forming phases across different classes of materials. Frank-Kasper phases have their origins in metallic alloys; the discovery of increasingly complicated crystal structures ultimately led to the development of general rules governing tetrahedral packing within these alloys by Frank and Kasper at the end of the 1950s.[19,20]

While Frank-Kasper phases remain most commonly found in such alloys, they also have been identified in an increasingly wide variety of soft matter in the past 30 years, including liquid crystals,[21–30] dendrimers,[31,32] sugar-polyolefins[33] and shape amphiphiles.[34–38] Is there an underlying mechanism governing the emergence of similar packing across such a wide variety of soft materials? If so, block polymers should prove to be the ideal system to probe those connections because block polymer thermodynamics are relatively straightforward and, in the long chain limit, have universal properties that simplify their description within a statistical mechanical framework.[5] An even more ambitious question is whether Frank-Kasper phase formation in soft matter, in particular block polymers, can shed any insights into the general principles governing their appearance in hard matter.[39] The third motivation concerns applications; both Frank-Kasper phases and related quasicrystals are expected to exhibit photonic bandgaps[40–44] that should be realizable in soft matter.[32] Compared to other soft matter that forms Frank-Kasper phases, block polymers produce the largest unit cell sizes,[45] making them the platform of choice in soft matter to push those band gaps into the visible range.[46] Such materials find applications in photonic systems that use light, rather than electrons, as the medium for information tranmission.[47] Frank-Kasper phases may also prove to be effective for enhancing ion transport.[48]

This Perspective provides a concise review of the current understanding of Frank-Kasper phase formation in diblock polymer melts, blends, and related multiblock polymer systems. This will reveal a few successes, most notably understanding the effects of conformational asymmetry and blending on the stabilization of Frank-Kasper phases. In many cases, these successes emerged from a synergistic combination of polymer synthesis, characterization, and the mean-field theory embodied in SCFT, the latter of which has been reviewed elsewhere.[49–53] We will also identify many open questions that are fruitful avenues for future investigation, in particular for cases where theory cannot yet provide anything beyond a qualitative explanation of some of the observed phenomena. Closing the gap between theory and experiment would enable rational approaches to both molecular design and processing

strategies that favor the formation of Frank-Kasper phases.

Frank-Kasper phases in block polymers

Frank-Kasper phases are tetrahedrally close-packed systems, meaning that each particle forms a tetrahedron with each of its nearest neighbors in the coordination shell.[19] The tetrahedra are distorted, which is required to make a periodic 3D packing. Tetrahedral close-packing is distinct from a close-packed structure such as fcc, where planes of spherical particles are touching, or phases with a compact direction like bcc, where spherical particles on the (111) direction are in contact. Tetrahedral packing produces Wigner-Seitz cells with coordination numbers, i.e. the number of faces on the Wigner-Seitz cell, of 12, 14, 15 and 16, which we will denote, for example, as Z12. Laves phases are a subset of Frank-Kasper phases with only Z12 and Z16 polyhedra.[54] The existence of multiple types of Wigner-Seitz cells contrasts with close-packed phases like fcc (one Z12 particle) and bcc (one Z14 particle; see Fig. 1).[19] Frank-Kasper phases are often found in metallic alloys, where the different coordination number positions allows the material to accommodate atoms with multiple preferred coordination numbers and different sizes. For example, the σ phase is found in binary and ternary systems of transition-group metals,[55] although having an alloy is not a requirement to form the σ phase, as exemplified by β-uranium[56] and β-tantalum.[57]

There are 27 known Frank-Kasper phases in metallic alloys, and many more proposed structures satisfy the rules for tetrahedral close-packing.[18] However, only four Frank-Kasper phases have been identified in block polymer systems: the σ phase,[17] the A15 phase,[59] and the Laves phases C14 and C15.[60,61] Figure 2 provides the unit cell structures for these phases, along with the Wyckoff positions of the particles, their space groups (which are often used to describe these phases, for example, in the liquid crystal literature[21–23,31]), and representative polyhedra formed from each particle type. Wyckoff positions are converted readily to unit cell coordinates using the Bilbao Crystallographic Server.[62]

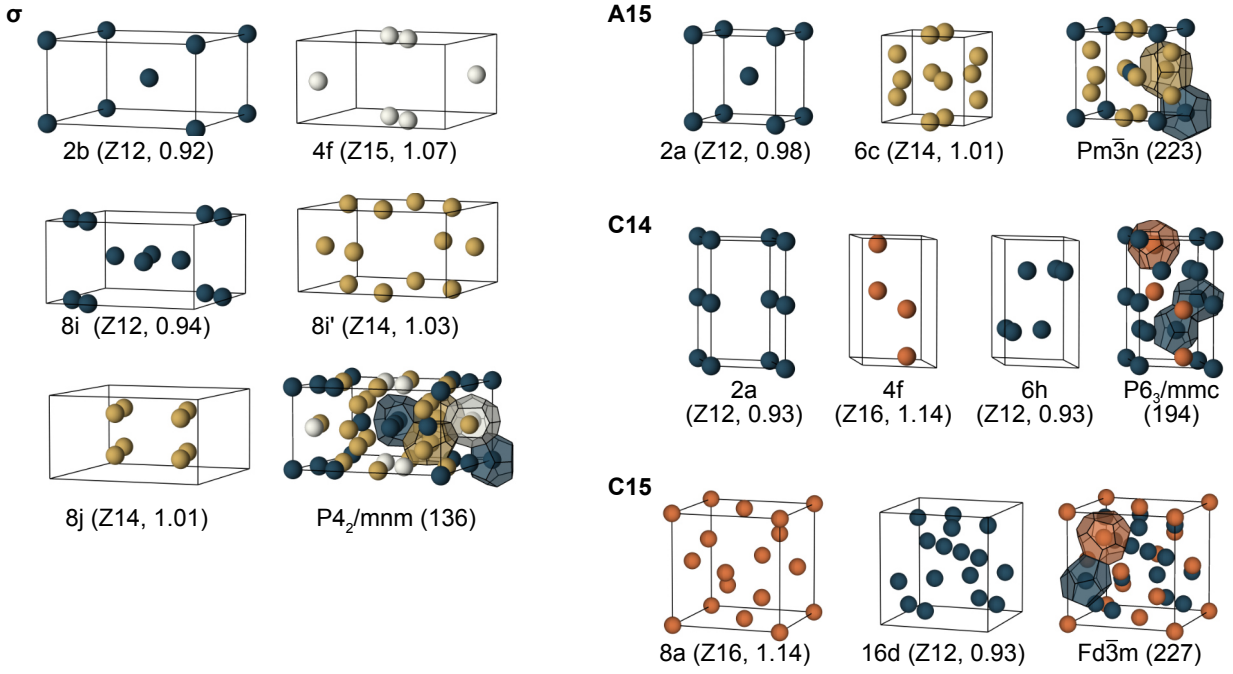

Figure 2: Illustration of the four Frank-Kasper phases found in block polymers. For each phase, the number of distinct particle types are displayed (σ = 5, A15 = 2, C14 = 3, C15 = 2) according to their Wyckoff positions. The parenthetical information provides the coordination number for the resulting polyhedron and the volume of that polyhedron relative to the number-averaged volume of the polyhedra for that phase. The image of the complete structure includes representative polyhedra for each particle type, along with the space group name and number. The aspect ratio of the σ phase is $a/c = 1.9$ and the crystal structure uses the coordinates in Ref. 55. The hexagonal C14 phase has an aspect ratio $c/a = 1.63$ and the crystal structure uses the coordinates in Ref. 58. The A15 and C15 structures can be constructed solely from their Wyckoff positions and space group symmetry without any additional coordinate information. Additional information about the crystallography of Frank-Kasper phases is provided in the Supporting Information of Ref. 4.

The σ phase, with a remarkably large unit cell consisting of 30 particles with five different particle types, is the most frequently observed Frank-Kasper phase in block polymers, having been identified experimentally in diblock copolymer melts,[17,39,59,63–68] ABA triblock copolymers,,[66] AB_n star copolymers,[66] miktoarm copolymers,[69,70] ABAC tetrablock terpolymers,[17,71] coil-bottlebrush polymers,[72] diblock copolymer/homopolymer blends with homopolymer added to the core[73] or to the matrix,[74,75] and in diblock copolymer blends.[76–78] As a curious historical note, the σ phase was undoubtedly produced by Papadakis and cowork-

ers[79] in a poly(ethylene-*alt*-propylene)-*b*-polydimethylsiloxane (PEP-PDMS) system in 1999, more than a decade before its definitive identification by Lee *et al.*[17] in poly(isoprene)-*b*-polylactide (PI-PLA); the confirmation of a σ phase in PEP-PDMS was only achieved recently.[68]

The σ phase is a periodic quasicrystal approximant (see Supporting Information), and often appears in soft materials systems that produce a dodecagonal quasicrystal (DDQC).[31,32,35,80,81] The connection between the σ phase and the DDQC has also been observed in experiments utilizing diblock copolymers,[63,64,67,68] ABAC tetrablock terpolymers,[71,82] coil-bottlebrush copolymers,[72] miktoarm copolymers,[70] and diblock copolymer blends,[76,78] where the σ phase tends to emerge slowly as the equilibrium state out of a metastable DDQC.[63] In addition to these three-dimensional realizations of the σ phase, the related $3^2.4.3.4$ Archimedian tiling of the constituent particles has been seen in a thin film of a triblock star polymer blend[83] and a tetrablock terpolymer,[84] as well as via graphoepitaxy of a diblock copolymer.[85] The related quasicrystalline tiling was also observed in the same triblock star polymer blend.[86] In these thin films, the polymers form cylinders oriented perpendicular to the surface, and the tiling reflects the complex two-dimensional ordering of the cylinders in the film. Theory predicts that this quasicrystalline tiling in a thin film is metastable.[87]

A15 is markedly simpler than σ, consisting of only two different types of particles, a Z12 and a Z14, arranged with a higher symmetry than the σ phase. A useful way to visualize the A15 phase is through the interstitial 2a sites, which form a bcc lattice, and a set of interlocking columns that enclose the 6j particles on the faces of the unit cell.[88] A15 has attracted considerable attention in soft matter in the context of foams, as it forms the basis for the Weaire-Phelan construction of a partition into equal volume cells of minimal surface area,[89] which will become important shortly when we consider the factors giving rise to Frank-Kasper phases in block polymers.[16] While less widespread than the σ phase, A15 has been identified in diblock copolymers,[59,66] ABA triblock copolymers,[66] AB_n star copolymers,,[66] miktoarm copolymers,[69,70,90] ABAC tetrablock terpolymers,,[71] coil-bottlebrush copolymers,[72] and di-

block copolymer blends.[76–78] Although the DDQC tends to evolve to σ, a DDQC to A15 transition was observed for bottlebush polymers[72] and diblock copolymer blends.[76]

C14 and C15 Laves phases have a particle stoichiometry of AB_2, where the A site is larger than the B site.[20] For this reason, the Wigner-Seitz cells in the C14 and C15 Laves phases in Fig. 2 have a larger volume asymmetry than the σ and A15 phases. The C14 and C15 phases correspond to different layerings of the A and B particles (see Supporting Information), and the similarities between C14 and C15 have analogies to the relationship between fcc and hcp packing. Compared to σ and A15, the C14 and C15 Laves phases are much harder to find in block polymers. Both phases are reported as the non-equilibrium phases in diblock copolymer melts following a deep quench in liquid nitrogen of the disordered liquid and subsequent heating,[60,65,91] and as equilibrium phases in (i) diblock polymer/homopolymer blends in the dry brush limit for homopolymer in the core[61,73] and (ii) AB/AB′ diblock copolymer blends.[78]

Mechanisms producing Frank-Kasper phases

Frank-Kasper phases have considerably lower symmetry than bcc ($Im\bar{3}m$, Space Group 239). Indeed, the most commonly observed Frank-Kasper phase in block polymers is the σ phase ($P4_2/mnm$, Space Group 136). In addition to lower lattice symmetry, Frank-Kasper phases have multiple particles that differ in size and shape. As such, the emergence of Frank-Kasper phases already violates the maxim that nature prefers states of higher symmetry.[4] In this section, we review the key factors associated with Frank-Kasper phase formation in block polymer systems, providing the context for the open questions raised in the following section.

Geometrical models

An early hypothesis on the stability of Frank-Kasper phases is that the system is maximizing the sphericity of the constituent polyhedra,[39] which can be quantified by the isoperimetric

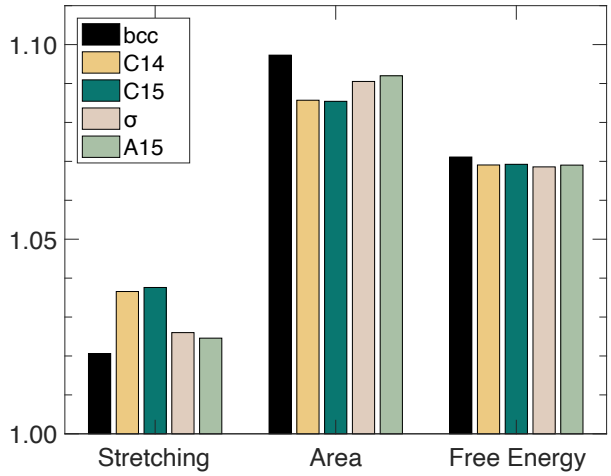

Figure 3: Dimensionless stretching moment $\mathcal{I}$, interfacial area $\mathcal{A}$ and free energy $\mathcal{F} = (\mathcal{A}^2\mathcal{I})^{1/3}$ computed from the unconstrained diblock foam model. These data are a subset of the results reported for 11 Frank-Kasper phases and bcc in Ref. 4.

coefficient

$$\mathrm{IQ} = \frac{36\pi V^2}{A^3} \tag{1}$$

where A is the area of the polyhedron and V is its volume; the prefactor 36π normalizes IQ such that IQ = 1 for a sphere. The IQ values of each symmetry-inequivalent particle in the Frank-Kasper phases observed in block polymers, as well as the number-averaged IQ, are provided in Table S1. The highest number-averaged sphericity (0.7624) is obtained for σ, followed by A15 (0.7617) and the C14 and C15 Laves phases (0.7613); importantly, all of these phases have higher number-averaged IQ values than bcc (0.7524). Thus, the sphericity theory based solely on the geometry of the Wigner-Seitz cells and a preference for forming the most spherical particles predicts σ as the equilibrium state.[39]

The principle of sphericity is purely geometric in origin, so it cannot capture in detail the enthalpic and entropic driving forces for selecting an ordered state in block polymers. The next level of complexity is the "diblock foam" model,[92,93] which is based on strong-stretching theory and the geometry of the Wigner-Seitz cells. The diblock foam approach was first pursued by Grason and coworkers[5,16] in the limit where each particle is constrained to have equal volume. The equal volume construction predicts A15 as a stable phase since

it makes the minimal area.[89] It is also possible to compute the free energy in the strong stretching limit while fixing the geometry of the Wigner-Seitz cells,[4] which would have unequal volumes (Fig. 2). Such a calculation expands the idea embedded in the sphericity theory[39] to explicitly account for the chain stretching and interfacial tension. However, the most illuminating strong stretching theory result considers a model where the particles are allowed to relax both their shape and size, thereby introducing mass exchange as part of the equilibration mechanism. Figure 3 reproduces a subset of the results from this unconstrained diblock foam model for the four Frank-Kasper phases observed in diblock copolymer melts, as well as bcc.[4] The minimal area is obtained by C15, whereas the minimal chain stretching is realized in bcc. (Note that, in Ref. 4, the minimal area for the unconstrained diblock foam calculation was incorrectly cited as C14.) The σ phase emerges as the equilibrium phase in the unconstrained diblock foam model because it provides the optimum balance between chain stretching and interfacial area.[4]

Conformational asymmetry

Conformational asymmetry, which quantifies the relative entropic penalty incurred by stretching two different blocks,[94] is a necessary condition for Frank-Kasper phase formation in neat diblock copolymer melts.[95] Generalizing a diblock copolymer to a star copolymer with n_i arms in each block with statistical segment length b_i, the conformational asymmetry is given by[96]

$$\epsilon = \frac{n_{\mathrm{B}}}{n_{\mathrm{A}}} \times \frac{b_{\mathrm{A}}}{b_{\mathrm{B}}} \tag{2}$$

where the statistical segment lengths are defined based on a common reference volume. (See Supporting Information for more details.) The first ratio is the architectural asymmetry that arises by replacing a single block of degree of polymerization N_i by n_i blocks with degree of polymerization N_i/n_i, which keeps the total volume fraction occupied by that moiety unchanged. In order to fill the space, these shorter chains need to stretch further,

which incurs an entropic penalty. The second ratio is the elastic asymmetry created by the Gaussian entropy of the blocks, which again reflects the penalty for stretching the chains from the interface to fill the space, an entropic penalty which is inversely proportional to the statistical segment length.[96,97] If we define A to be the minority block with volume fraction $f_A < 1/2$, Frank-Kasper phases emerge when $\epsilon > 1$.[5,16,95]

Note that the equivalence between changing the statistical segment lengths and changing the number of arms is only valid in the strong-stretching limit of large χN. For lower χN, in particular in weakly segregated systems, the differences in elastic and architectural asymmetry become sensible due to the different ways to pack the linear and branched chains when they are not making radial trajectories away from the interface; these impacts are well illustrated in their effects on the diblock phase diagram.[98]

Conformational asymmetry favors curvature towards the large b_i block, which provides space on the convex side of the interface for block incurring the larger stretching penalty to relax.[99] Interfacial curvature is also favored by compositional asymmetry, so one can imagine, to a first approximation, that increasing ϵ is similar to reducing f_A.[99] As a result, there is a right-skew of the overall phase diagram, which is borne out in both strong-stretching theory[93,96] and SCFT calculations.[100] The Supporting Information provides a relatively simple way to understand this shift in terms of ϵ, inspired by the polymer brush model of Milner,[96] which also furnishes a straightforward way to recognize the equivalence of architectural and elastic asymmetries embodied in Eq. 2. The net effect is to stabilize particle-forming phases at higher volume fractions f_A of the minority A-block, which increases the relative core volume and interfacial area.

This shift in the phase diagram was a key step to the first prediction of an A15 phase illustrated in Fig. 4;[16] for linear diblock copolymers, A15 overtakes bcc and fcc as the most stable particle-forming state in the hex cylinder region, and skewing the phase diagram using a multiply branched polymer allows A15 to become the stable state before the transition to the cylinder-forming region. Increasing ϵ for compositionally asymmetric polymers also

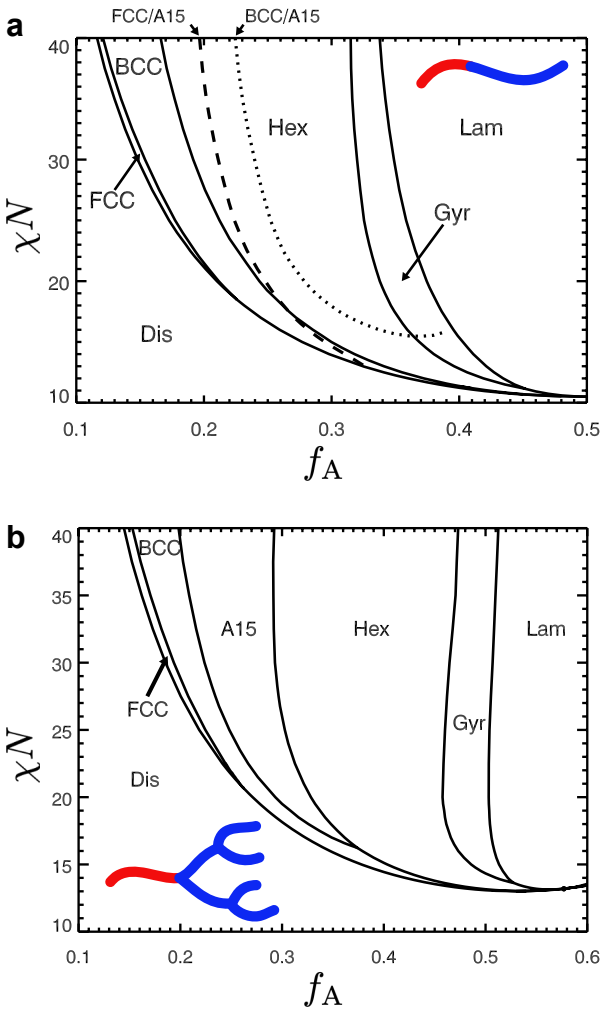

Figure 4: SCFT calculation[16] of the phase diagram for (a) linear diblock polymer melt and (b) a three-generation branched polymer melt. The dashed lines in (a) refer to crossovers in free energy for metastable particle-forming phases. Gyr = double gyroid, Lam = lamellar, Dis = disorder. The σ phase was not included as a candidate phase in these calculations since it was discovered seven years later;[17] its inclusion as a candidate phase leads to σ overtaking A15 at modest conformational asymmetry.[59,95] Adapted with permission from Grason, G. M.; DiDonna, B. A.; Kamien, R. D. Geometric Theory of Diblock Copolymer Phases. *Phys. Rev. Lett.* **2003**, *91*, 058304. Copyright 2003 American Physical Society.

penalizes stretching of the matrix chains. This leads to an imbalance in the chain stretching energy such that the corona chains, which need to stretch to reach the corners of the Wigner-Seitz cell, exert a force on the interface that causes the transition in the cylindrical domain shown in Fig. 5 from a circular shape to a polyhedral shape that reflects the shape of the Wigner-Seitz cell; the equivalent three-dimensional distortion for a micellar particle is from a

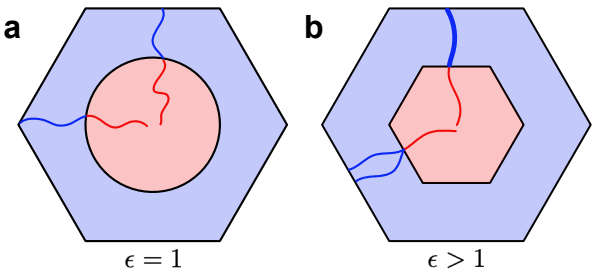

Figure 5: Effect of conformational asymmetry on the AB interface, illustrated here for the case of hexagonally-packed cylinders (hex). (a) For $\epsilon = 1$, the mechanical force due to stretching is balanced and the system prefers a circular AB interface. (b) Polyhedral imprinting is preferred for $\epsilon > 1$ to relieve the chain stretching penalty incurred by corona chains that need to reach the corners of the Wigner-Seitz cell. The extreme situation of perfect imprinting illustrated here is the polyhedral interface limit,[5] which would be the case for large ϵ and also appears in the straight chain ansatz used in the diblock foam model.[92,93]

spherical shape to a polyhedral one,[5] although this idea is somewhat more complicated when the confining shapes are the polyhedra of the Wigner-Sietz cells.[4] In the limit of large ϵ, we would expect to realize the polyhedral interface limit illustrated in Fig. 5. The polyhedral interface limit is also used in the diblock foam model[4,5] because, in the strong-stretching limit, the chains tend to adopt straight paths away from the interface,[92,93] independent of ϵ.

Taken together, these two effects of conformational asymmetry lead to an increasing role of the shapes of the Wigner-Seitz cells on particle packing as the conformational asymmetry increases.[5,16] Frank-Kasper phases are desirable in this respect, since their higher average sphericity[39] provides smaller interfacial areas in the polyhedral interface limit.[4,5,16] SCFT calculations, reproduced in Fig. 6, illustrate how the Frank-Kasper stability window, and in particular the A15 stability window, gradually widens with increasing conformational asymmetry.

The qualitative picture of Fig. 6 is consistent with almost all experiments on diblock copolymer melts:[17,39,59,63–68] an initial emergence of σ with increasing conformational asymmetry followed by the appearance of A15 at higher f_A when the conformational asymmetry increases further. There are two notable exceptions to this trend. The first are experiments using linear and miktoarm architectures of discrete oliogomeric dimethylsiloxane and lactic

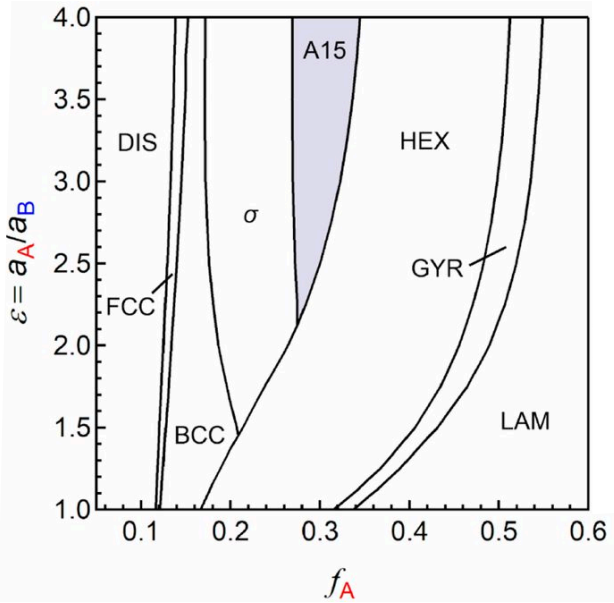

Figure 6: SCFT phase diagram[59] at $\chi N = 40$ as a function of the conformational asymmetry ϵ and the compositional asymmetry f_A. Adapted with permission from Bates, M. W.; Lequieu, J.; Barbon, S. M.; Lewis III, R. M.; Delaney, K. T.; Anastasaki, A.; Hawker, C. J.; Fredrickson, G. H.; Bates, C. M. Stability of the A15 phase in diblock copolymer melts. *Proc. Natl. Acad. Sci. USA* **2019**, *116*, 13194–13199. Copyright 2019 National Academy of Sciences.

acid, where the compositions were resolved to the single monomer level.[70] The conformational asymmetry of the linear diblock oligomer is $\epsilon = 1.46$ but the compositional asymmetry of the library used in these experiments was insufficient to observe a particle-forming window at this value of ϵ. Adding additional arms of the majority block shifts the phase diagram due to conformational asymmetry and opens up a particle-forming window. The value $n_B = 2$ ($\epsilon = 2.92$) produces an A15 phase, with the σ phase only emerging when $n_B = 4$ ($\epsilon = 5.84$). A likely reason for this behavior is the relatively low degrees of polymerization used in these experiments, which cuts off the bottom of the SCFT phase diagram with a disordered state, and the particular values of f_A, which may not be low enough for $n_B = 2$ to produce a σ phase. The second exception is the observation a C14 phase in poly(dimethylsiloxane)-*b*-poly(2,2,2-trifluoroethyl acrylate) (PDMS-*b*-PTFEA) diblock copolymer that is located between the bcc and σ phases with increasing f_A.[65] The scattering data reported from the PDMS-*b*-PTFEA experiments, which clearly indicates the presence of a C14 phase, produce

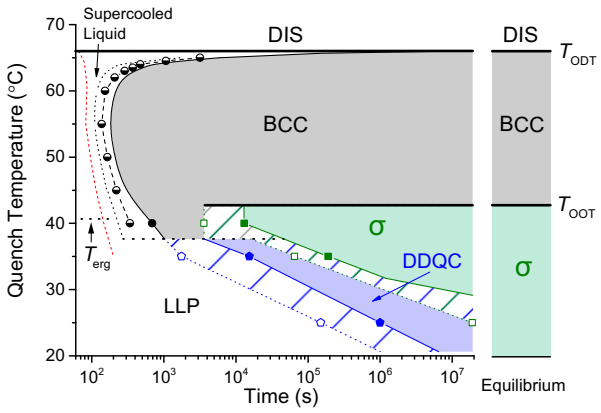

Figure 7: Time-temperature-transformation diagram[63] for a poly(isoprene)-*b*-poly(lactide) diblock copolymer melt. LLP = liquid-like packing. The temperature T_{erg} denotes the point at which quenches below T_{erg} produce non-ergodic behavior. Reproduced with permission from Gillard, T. M.; Lee, S.; Bates, F. S. Dodecagonal quasicrystalline order in a diblock copolymer melt. *Proc. Natl. Acad. Sci. USA* **2016**, *113*, 5167–5172. Copyright 2016 National Academy of Sciences.

a sequence of phases different than those seen in Fig. 6 and other experiments.[17,39,59,63–68] Determining the mechanism by which PDMS-*b*-PTFEA produces a C14 phases remains an interesting open question for future work.

Thermal processing

To date, the only equilibrium Frank-Kasper phases reported for neat diblock copolymer melts are σ and A15. However, through control of the thermal history of the sample, it is possible to access metastable states.

Figure 7 provides the first illustration of the effect of thermal processing on Frank-Kasper phase formation, focusing on a block polymer similar to the PI-PLA system used for the discovery of the σ phase[17] but at a molecular weight that provides a larger temperature window between the order-disorder transition and the glass transition temperature for the PLA block.[63] Modest temperature quenches out of the disordered state produce bcc, but more complex time-dependent behavior emerges for deeper quenches, producing bcc-to-σ and DDQC-to-σ order-order transitions. In this case, the DDQC forms from a liquid-like packing state (LLP), which is characterized by a broad primary peak in the scattering (Fig. 8b) and

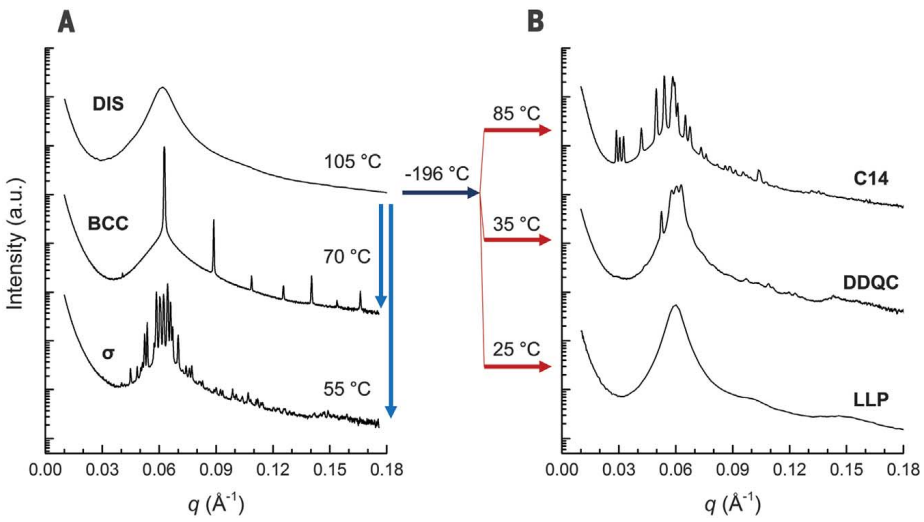

Figure 8: Illustration of the effect of thermal processing on ordered state selection in a poly(isoprene)-*b*-poly(lactide) diblock copolymer melt with $f_A = 0.15$.[60] (a) Cooling the sample slowly. (b) Deep quenching in liquid N_2 followed by heating to a target temperature. Reproduced with permission from Kim, K.; Schulze, M. W.; Arora, A.; Lewis III, R. M.; Hillmyer, A.; Dorfman, K. D.; Bates, F. S. Thermal Processing of Diblock Copolymer Melts Mimics Metallurgy. *Science* **2017**, *356*, 520–523. Copyright 2017 American Association for the Advancement of Science.

likely arises due to kinetic trapping. The details of LLP remain a poorly understood aspect of block polymer assembly, and a later part of this discourse will highlight several open questions related to LLP that are worth further investigation. The emergence of a DDQC prior to σ may bear some similarities to simulations of colloidal quasicrystals.[101,102] Since the DDQC is created from the same square and triangular tiles as σ (see Supporting Information), it is plausible that the DDQC represents a way for the system to first form the requisite tiles, which then reorganize themselves into the equilibrium, periodic σ phase.[102]

Thermal processing also provides a route for accessing the C14 and C15 Laves phases as metastable states.[60] As illustrated in Fig. 8, cooling a PI-PLA diblock copolymer melt with $f_A = 0.15$ from disorder produces bcc and then σ, behavior that would be anticipated from the SCFT phase diagram.[95] However, if the system is quenched from the disordered state in liquid nitrogen and then reheated, different morphologies are selected based on the degree of heating, including C14, without accessing bcc or σ.[60] A similar processing strategy, using a

higher value of $f_A = 0.20$, produces C15 instead of C14.[60] Presumably, the deep quenching traps the distribution of micelles from the disordered state (or some related state achieved during the cooling process), which then templates the formation of the ordered state within a rough free energy landscape after heating.[60] The appearance of Laves phases via thermal processing may be related to their large volume asymmetry that must achieved from an initially more narrow distribution of particle sizes via mass transfer.[4]

The thermal processing conditions connected to Laves phase formation are even more complicated than the "simple" deep quench process illustrated in Fig. 8. Subsequent experiments[91] demonstrated that these systems retain memory of the metastable ordered state after crossing the order-disorder transition. In other words, after a thermal processing path that leads to the C14 state in Fig. 8b, returning the material to the disordered state does not recover the processing path of Fig. 8a. Rather, after disordering a metastable C14 (or C15) state, subsequent cooling will reform the same metastable ordered state, even though the relaxation times, measured by rheology, are much faster than the thermal processing time.[91]

Blending

Neat diblock copolymer melts already exhibit a rich picture of Frank-Kasper phase formation, especially in light of the simplicity of the molecules, producing equilibrium σ and A15 phases and permitting the formation of metastable Laves phases and a DDQC through thermal processing. To access more equilibrium Frank-Kasper phases, as well as widen their stability windows, it is necessary to introduce additional complexity to the system. In a sense, the examples we have seen before are the polymer equivalents to the few cases where single component metals form Frank-Kasper phases.[56,57] In hard materials, Frank-Kasper phases are observed more broadly in alloys that readily permit multiple particle sizes. Blending, using either mixtures of block copolymers[76,77,103] or doping the system with homopolymer,[73,104–107] is an analogous "alloying" approach for block polymers.

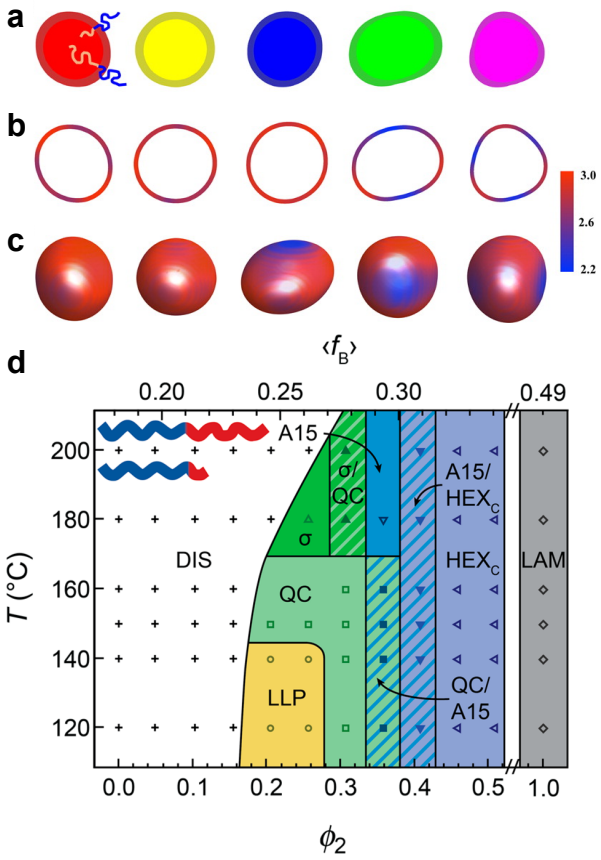

Figure 9: Formation of Frank-Kasper phase in diblock/diblock copolymer blends.[76,103] (a) Different size diblock copolymers preferentially segregate to different faces of the polyhedra in the σ phase. (b) SCFT predictions of the location of the AB junction points for the diblock copolymer with the shorter A-block on a plane. (c) Same as (b) but in three dimensions. (d) Experimental phase diagram for a blend of poly(styrene)-*b*-1,4-polybutadiene (SB) where the corona blocks are identical but the core blocks differ (1 = smaller core block). The quantity $\langle f_B \rangle$ refers to the volume fraction of the minority butadiene block in the mixture. Panels (a)-(c) reproduced with permission from Liu, M.; Qiang, Y.; Li, W.; Qiu, F.; Shi, A.-C. Stabilizing the Frank-Kasper phases via binary blends of AB diblock copolymers. *ACS Macro Lett.* **2016**, *5*, 1167–1171. Copyright 2016 American Chemical Society. Panel (d) reproduced with permission from Lindsay, A. P.; Lewis III, R. M.; Lee, B.; Peterson, A. J.; Lodge, T. P.; Bates, F. S. A15, σ, and a Quasicrystal: Access to Complex Particle Packings via Bidisperse Diblock Copolymer Blends. *ACS Macro Lett.* **2020**, *9*, 197–203. Copyright 2020 American Chemical Society.

The proposed mechanism for stabilizing Frank-Kasper phases in diblock polymer blends, illustrated in Fig. 9a, involves forming a core-shell structure with the core comprised primarily by the longer blocks, which can more easily stretch to the center of the particle, while the short blocks form the shell.[103] Only a small amount of long copolymer was sufficient to

produce a σ to bcc transition in SCFT, and wide σ and A15 windows were predicted for the blended systems even when the block polymers are conformationally symmetric.[103] In addition to allowing for different amounts of polymer per particle, SCFT predicts a segregation of the different polymers along the interface, with the more compositionally symmetric molecules preferring the flatter interfaces and vice versa.[103]

The key predictions of SCFT were realized experimentally as shown in Fig. 9d, where binary blends of poly(styrene)-*b*-1,4-polybutadiene (SB) with one component containing a short B core block (which is disordered as a single-component melt) and a second polymer with a longer core block (which forms lamellae as single-component melt) produce all of the phases seen in neat diblock copolymer melts: A15, σ and DDQC.[76] The qualitative behavior observed in Fig. 9d has also been reproduced in a polystyrene-*b*-poly(methyl acrylate) system.[77] Subsequent work with the SB system, using higher molecular weight polymers such that the short core block now forms bcc as a single-component melt, yielded not only A15, σ and DDQC, but also produced a C14 phase when a small amount of lamellar-forming SB was blended into the bcc-forming polymer.[78] Related experiments using three different blends, using the same strategy of keeping the majority block lengths fixed and varying the ratio of the core block length, revealed that the Frank-Kasper phase window widens as the spread in the relative lengths of the core blocks increases.[78]

Blending of block polymers with homopolymers, where the homopolymer is chemically identical to one of the blocks, is another way to stabilize new phases in block polymers. In many cases, the effect of homopolymer is to relieve packing frustration by allowing the homopolymer to segregate to the most frustrated regions.[108] Homopolymer blending is generally classified into two regimes. In the wet brush regime,[109] the added homopolymer has a degree of polymerization that is smaller than the chemically identical block, which allows the homopolymer to interpenetrate the block and wet the interface. In contrast, a dry brush regime[109] is realized when the homopolymer is at least of similar length to the block. The homopolymer then tends to be segregated from the homologous block.

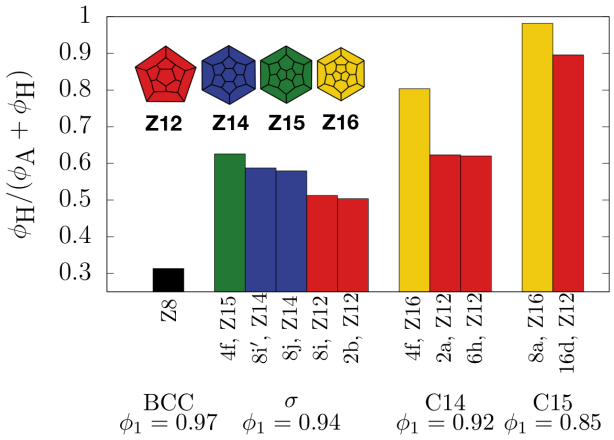

Figure 10: SCFT predictions[106] for the extent of homopolymer partitioning into different particles for volume fractions ϕ_1 of block polymer where the indicated phase is stable in SCFT. Reproduced with permission from Cheong, G. K.; Bates, F. S.; Dorfman, K. D. Symmetry breaking in particle-forming diblock polymer/homopolymer blends. *Proc. Natl. Acad. Sci. USA* **2020**, *117*, 16764–16769. Copyright 2020 National Academy of Sciences.

Wet brush blending is tends to stabilize the same Frank-Kasper phases seen in neat block polymer melts.[73,104] In contrast, dry brush blending of core block homopolymer produces not only a σ phase, but also equilibrium C14 and C15 phases.[73] The initial rationale for this sequence was a relief of core-block packing frustration and the ability of the homopolymer to facilitate formation of particles of different sizes.[73] Subsequent SCFT calculations[106,107] have revealed a more nuanced picture of the stabilization mechanism. As illustrated in Fig. 10, the homopolymer tends to partition into the larger (higher coordination number) particles within a given phase. The Laves phases emerge at the higher homopolymer loading because they possess greater volume asymmetry than σ, and thus can accommodate more homopolymer without separating into two phases. Likewise, the absence of A15 was explained by its minimal volume asymmetry,[106] although there is speculation[107] that a higher conformational asymmetry would drive the formation of A15 in this system as well.

The SB system that produces the Laves phases in a homopolymer/block polymer blend[73] has a conformational asymmetry $\epsilon = 1.3$, which is too low to form any Frank-Kasper phases as a neat melt (Fig. 6). SCFT predicts the bcc-σ-C14-C15 phase sequence for both $\epsilon = 1.3$ and for the conformationally symmetric case $\epsilon = 1$,[106,107] demonstrating that this volume

asymmetry mechanism is not predicated on any additional stabilization of the Frank-Kasper phases by conformational asymmetry. However, SCFT predicts that dry brush homopolymer loading can be combined with the high conformational asymmetry embodied in AB_4 miktoarms to force systems that would otherwise form σ or A15 to transition to a Laves phase.[105]

Matrix segregation in multiblock polymers

Multiblock polymers provide another route to introduce additional complexity beyond the neat diblock copolymer melt, maintaining the single component nature and thereby suppressing the complication of macroscopic phase separation in multicomponent systems. In this context, the poly(styrene)-*b*-poly(isoprene)-*b*-poly(styrene)-*b*-poly(ethylene oxide) (SIS′O) tetrablock terpolymer system has been at the vanguard of Frank-Kasper phase discovery in block polymers, appearing in the first report of the σ phase,[17] the first DDQC observed in block polymers,[82] and the first A15 phase.[71] Manipulating the relative degree of polymerization between the terminal S-block (N_{S}) and the interior S′-block ($N_{\mathrm{S}'}$) provides a way to tune the phase behavior, with experiments using the asymmetry $\tau = N_{\mathrm{S}}/(N_{\mathrm{S}} + N_{\mathrm{S}'}) = 0.73$ unveiling a cornucopia of sphere-forming phases, including A15, σ, a DDQC, and two still unexplained phases, one with rhombohedral symmetry and an apparent hexagonal packing of spheres.[71]

The SIS′O system can be described as a pseudo-diblock system,[1] where the relatively strong segregation embodied in χ_{SO} and χ_{IO} compared to the modest segregation captured by χ_{IS} leads to the I- and S-blocks to form a relatively well mixed matrix with strong segregation with the O-block. By making the volume fraction of the O-block small, the system forms spheres of O whose interactions are tuned by the details of the matrix interactions.[71,82] Figure 11a illustrates how those interactions promote the formation of an A15 phase, with SCFT calculations revealing how the interior S′-block forming a core around the particles and the terminal S-block segregating within the matrix to guide the O-spheres onto the

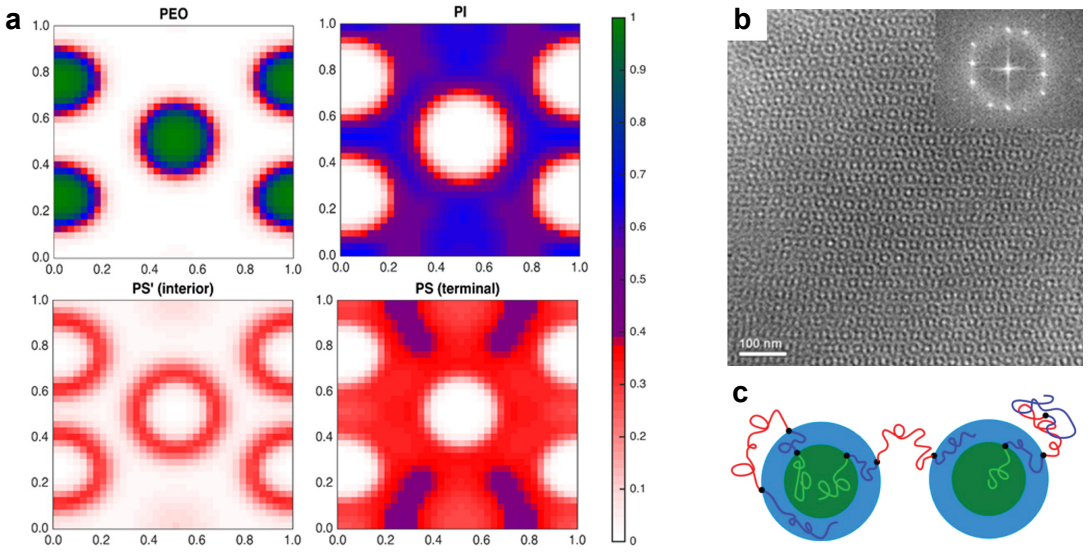

Figure 11: Formation of the A15 phase in an SIS′O tetrablock terpolymer.[71] (a) SCFT predictions for the distribution of the different blocks on the xy plane at $z = 1/2$ for $\tau = 0.73$. (b) TEM image of the A15 phase for $\tau = 0.70$. The inset is the Fourier transform of the image. (c) Looping and bridging configurations of the multiblock polymer. Reproduced with permission from Chanpuriya, S.; Kim, K.; Zhang, J.; Lee, S.; Arora, A.; Dorfman, K. D.; Delaney, K. T.; Fredrickson, G. H.; Bates, F. S. Cornucopia of Nanoscale Ordered Phases in Sphere-Forming Tetrablock Terpolymers. *ACS Nano* **2016**, *10*, 4961–4972. Copyright 2016 American Chemical Society.

A15 lattice. Figure 11b further illustrates an important advantage of the SIS′O system in practice; the staining contrast of the blocks makes it well suited to TEM imaging, allowing an unambiguous identification of the A15 tiling pattern. The key to the phase behavior is the terminal S-block (Fig. 11c), which can directly link two particles via a bridge, dangle within the matrix (leading to the matrix segregation effect in Fig. 11a), or loop back to swell the S-shell around the O-spheres.[110] The looping effect is responsible for the formation of σ in this class of tetrablock terpolymers in the absence of any conformation asymmetry because it increases the interfacial area and accentuates the tendency to favor the more spherical interface, and thus the σ phase.[110]

While the SIS′O tetrablock terpolymer has been the focus of experimental studies of Frank-Kasper phase formation in multiblock polymers,[17,71,82] other promising multiblock architectures have been proposed and studied by SCFT.[111–115] A particularly intriguing

candidate is the $B_1AB_2CB_3$ pentablock terpolymer, where the subscripts indicate the B-blocks are all of different degrees of polymerization. This system has been analyzed by SCFT for the case where the Flory-Huggins parameters between chemically dissimilar blocks are equal and large ($\chi N = 80$).[111] It is predicted to form a large number of particle-forming phases, include many low-coordination number phases that mimic metallic crystals, as well as the high-coordination number A15 phase. An important characteristic of this pentablock system is that, since all blocks are equally incompatible, using relatively low volume fractions of the A and C blocks forces the formation of two different sized particles, a key element of Frank-Kasper phases.

Key outstanding questions

Clearly, there has been substantial progress in the past decade towards understanding the mechanisms underlying Frank-Kasper formation. For neat diblock copolymer melts, conformational asymmetry proves to be the key element in stabilizing the σ and A15 phases,[5,16,59,95] and metastable DDQC and Laves phases can be accessed via thermal processing routes.[60,63,91] The additional complexity afforded by blending and multiblock polymers can be used to widen the σ and A15 windows[71,76,77] via spatial segregation between chemically similar blocks,[71,103] and can produce stable C14 and C15 phases[73] by swelling the particle cores in an analogy with the same mechanism operative in lyotropic liquid crystals.[26] There are, as always, technical details that need to be addressed within the context of these results and arguments that would be sharpened by additional experimental or theoretical evidence. In the interest of conciseness, we eschew these issues here to focus instead on several substantial questions, some of which have been raised elsewhere,[116] that should prove to be fruitful areas of future work.

The conformational asymmetry conundrum

There is no doubt that conformational asymmetry is a prerequisite for Frank-Kasper phase formation in neat diblock copolymer melts, and the trend in the phase progression in Fig. 6 agrees qualitatively with experiments. However, the degree of conformational asymmetry anticipated by SCFT is markedly higher than that needed in experiments and this difference remains an important unresolved issue. Figure 12 provides a particularly compelling comparison between experiments and SCFT predictions. In the experimental data of Fig. 12a, the σ phase window is sensible already at $\epsilon = 1.15$ and but only achieves a similar width in the SCFT data of Fig. 12b at $\epsilon = 2.0$. There are also qualitative differences between the experiment and SCFT that are anticipated from fluctuation effects that are not captured by the mean field theory, most notably the cutoff of the lower part of the phase diagram.[117,118] This is not an isolated example; similar quantitative disagreements between the requisite conformational asymmetry predicted by SCFT and experiments have been observed for the A15 phase in both diblock copolymers[59] and AB_n radial star polymers.[66] For example, the A15 phase for volume fractions f_A between 0.25 to 0.33 in a poly(dodecyl acrylate)-*b*-poly(lactide) (DL) melt emerges at $\epsilon = 1.85$, well below the SCFT prediction in Fig. 6.[59]

A possible explanation for this disagreement may come from the propensity to form Frank-Kasper phases as the invariant degree of polymerization $\bar{N} = Nb^6/v^2$ decreases, where v is the segmental volume. This phenomenon was exposed by experiments using a SB system[119] with a conformational asymmetry $\epsilon = 1.30$ that is the same, to within experimental uncertainty, to the PEE-PLA system[64] in Fig. 12a, but at a higher $\bar{N}$. In contrast to the results in Fig. 12a, experiments at a higher $\bar{N}$ failed to produce a σ phase, consistent with SCFT predictions (Fig. 6), which assume $\bar{N} \to \infty$.[119] Indeed, even blending of two SB diblock polymers with modestly different degrees of compositional asymmetry did not lead to a σ phase in this SB system.[119] Interestingly, the mean-field behavior is achieved when the invariant degree of polymerization of the individual blocks is above $\bar{N}_x \approx 400$,[119] which is approximately the degree of polymerization at the entanglement crossover that produces a

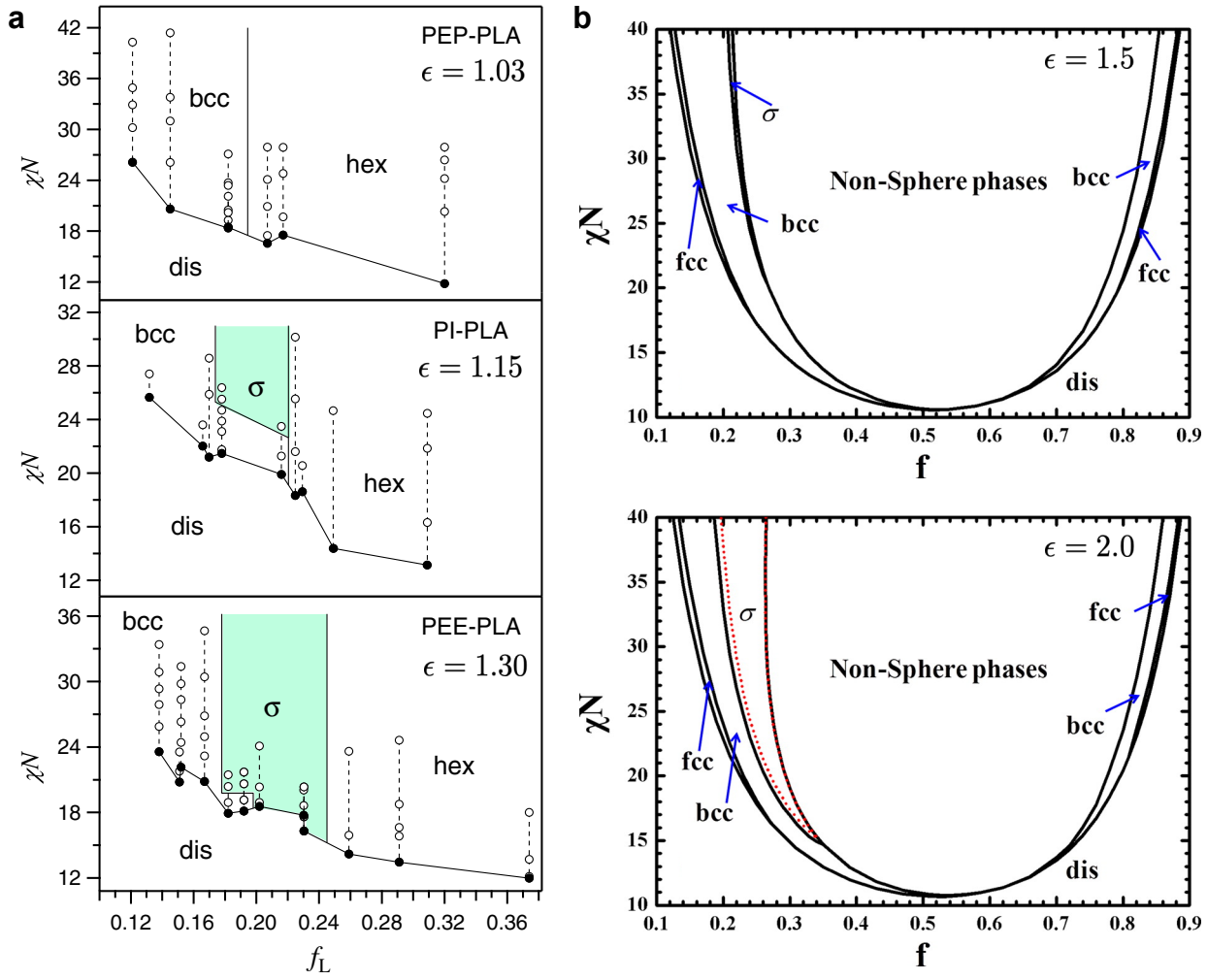

Figure 12: Comparison between experimental data[64] and SCFT calculations[95] for the emergence of the σ phase with increasing elastic asymmetry. (a) Experimental data[64] for three different block polymers where the minority block is poly[(±)]-lactide and the majority blocks are poly(ethylene-*alt*-polypropylene) (PEP), poly(isoprene) (PI) or poly(ethylethylene) (PEE). The values of ϵ appearing in Ref. 64 have been converted to the convention in Eq. 2. $\bar{N}$ values range from 130 to 510. (b) SCFT calculations[95] at $\epsilon = 1.5$ (top) and $\epsilon = 2.0$ (bottom). Panel (a) adapted with permission from Schulze, M. W.; Lewis III, R. M.; Lettow, J. H.; Hickey, R. J.; Gillard, T. M.; Hillmyer, M. A.; Bates, F. S. Conformational Asymmetry and Quasicrystal Approximants in Linear Diblock Copolymers. *Phys. Rev. Lett.* **2017**, *118*, 207801. Copyright 2017 American Physical Society. Panel (b) reproduced with permission from Xie, N.; Li, W.; Qiu, F.; Shi, A.-C. σ phase formed in conformationally asymmetric AB-type block copolymers. *ACS Macro Lett.* **2014**, *3*, 906–910. Copyright 2014 American Chemical Society.

shift from Rouse to reptation dynamics, and also the value of $\bar{N}$ where renormalized one-loop theory fails to capture simulation data for the order-disorder transition temperature.[120–122]

One issue that has been posed at low $\bar{N}$ is that polydispersity might play a role in stabilizing Frank-Kasper phases.[91] For example, the PI-PLA system used to discover the Laves phases[60] has a PLA block that is between 7-9 repeat units. As a result, differences in one repeat unit would create substantially different compositional asymmetries, which ultimately would look like a (relatively complicated) blend.[91] However, it is worth recalling that experiments using discrete oligomers[70] laid to rest the question of whether polydispersity is a necessary condition for Frank-Kasper phase formation at low $\bar{N}$; it is not.

It is not clear yet whether the strong fluctuation effects that become manifest at small $\bar{N}$ can also explain the conformational asymmetry conundrum. A systematic study of the effect of $\bar{N}$ is needed here, either experimentally or computationally. For the latter, field theoretic simulations[123–132] should prove useful provided that a sufficiently large system can be studied and sufficiently low $\bar{N}$ values can be reached. More generally, it is worthwhile to understand more deeply the implications (if any) of this intriguing connection between self-concentration, the crossover point of entanglement dynamics and the onset of mean-field behavior,[119] which remains relatively unexplored both in the context of Frank-Kasper phase formation or as a more general principle in polymer physics.

In addition to conformational asymmetry, the detailed packing of pendant side chains in bottlebrush architectures poses another open question related to conformational asymmetry and Frank-Kasper phase formation. In particular, the A15 phase in neat diblock copolymer melts requires a large conformational asymmetry, which has been achieved using the aforementioned DL system[59] and polynorbene-based polymers.[72] Both of these systems produce a coil-brush type architecture due to the pendant alkyl chain on one of the blocks. The modeling of the DL system treated the brush block as a Gaussian chain with a higher statistical segment length,[59] which captures the stiffness of the block but does not provide any details of the way the pendant chain is organized in space. While the increased stiffness is certainly the leading-order effect caused by the brush-like architecture, one should be careful in discounting the packing effect when the free energies of different competing phases

are very close,[59,60] and this may be one of the factors contributing to the need for SCFT to use a value of $\epsilon = 3$ to capture experimental data for $\epsilon = 1.85$.[59] From an applications standpoint, understanding Frank-Kasper phase formation in coil-brush architectures is especially important because bottlebrushes enable larger domain sizes that would be useful for optical applications, as has already been shown for lamellar phases in bottlebrush block polymers.[133–136]

What is liquid-like packing?

The thermal processing methods for stabilizing Frank-Kasper phases offer tremendous opportunities for discovery,[60,91] but further advances in this direction are not low hanging fruit. From a modeling standpoint, there exist powerful tools for understanding the pathways between ordered states.[137,138] A substantial challenge in applying these tools to Frank-Kasper phase formation are the enormous unit cells characterizing these phases, which require very large simulation cells. However, in the absence of any theoretical guidance, even at the qualitative level that we saw previously in the context of sphericity and conformational asymmetry, it is not clear how to proceed experimentally either.

Perhaps the most attractive entry point to addressing thermal processing is to understand the structure of the liquid-like packing (LLP) state that is produced by rapid quenching of the disordered material, although this likely requires a computational approach versus more experimentation due to the inherent challenges of inferring the micelle distribution from scattering. It is plausible that the LLP state has local tetrahedral packing within its structure.[39] This local structure could spawn either a DDQC or a Frank-Kasper phase by serving as a nucleation seed that grows to reach increasingly longer length scales. Simulating this behavior akin to what has been done for quasicrystal growth from a σ phase seed in colloids[102] would allow one to determine whether layers form first followed by tiling with rotational symmetry, or if a different pathway is selected. Another important question is whether the local tetrahedral ordering is already present in the disordered state, in particular

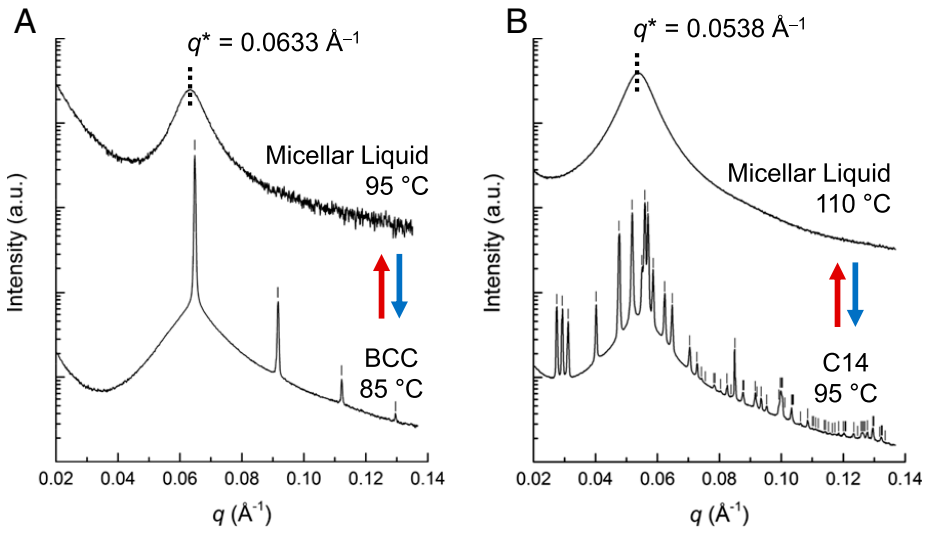

Figure 13: Memory effect of processing across the order-disorder transition for a PI-PLA system with $f_A = 0.15$.[91] (a) Freeze-drying, heating to 95 °C and the repeatedly cycling between 85 °C and 95 °C leads to bcc-disorder transitions. (b) Freeze-drying, heating to 95 °C, immersing in liquid nitrogen, heating to 95 °C, and then repeatedly heating to 110 °C and cooling to 95 °C produces C14-disorder transitions. Similar behavior using a polymer with $f_A = 0.20$ produces C15. Reproduced with permission from Kim, K.; Arora, A.; Lewis, R. M.; Liu, M.; Li, W.; Shi, A.-C.; Dorfman, K. D.; Bates, F. S. Origins of low-symmetry phases in asymmetric diblock copolymer melts. *Proc. Natl. Acad. Sci. USA* **2018**, *115*, 847–854. Copyright 2018 National Academy of Sciences.

for conformationally asymmetric systems, or whether it is formed as part of the quenching process. The former question does seem tractable from a simulation standpoint, either using coarse-grained molecular dynamics of a calibrated model[120,122,139,140] or through field theoretic simulations,[123–132] again provided that a sufficiently large system can be studied.

A second entry point of interest from the theory side is the memory of the metastable disordered state after processing across the order-disorder transition seen in Fig. 13. The memory effect appears in the scattering data in Fig. 13 as a shift in the primary peak of the disordered micellar liquid, but the underlying structure of that liquid is unknown. A hypothesis about the path-dependent structure formation is that there is a hierarchy of time scales as the system relaxes towards the equilibrium disordered state, with the single peak observed in the scattering of the disordered state[91] masking some local ordering that favors re-formation of the metastable Laves phase, rather than bcc. There must be a time scale at

which the material completely disorders, restoring the presumably equilibrium pathway in Fig. 8a. It is relatively straightforward to prepare a simulation in the metastable Laves phase; if the free energy landscape is as rough as postulated from the experimental dynamics,[60] the metastable state should be persistent. One could then impose an instantaneous temperature jump in the simulation and observe the resulting structural evolution. The computational challenges outlined in the context of LLP remain an issue here, with the need to simulate a large system. Indeed, this pathway problem is likely even more challenging than solely trying to interrogate the structure of the disordered state since it also requires temporal data on the order-disorder transition and may require long simulation times.

Given these computational limits, there is also merit in revisiting the experimental approach[91] and determining the time scale over which the micellar liquid primary peak in Fig. 13b evolves to that in Fig. 13a. There is already evidence that the ordering kinetics are very slow upon cooling, although the origin of the slowdown is not clear.[68] These slow dynamics may also extend to the transitions of LLP in the disordered state.

Panacea or Pandora's box revisited

Blending and multiblock polymers have proven already to be powerful platforms for expanding the palette of Frank-Kasper phases, both for theoretical predictions[71,103,105–107,110–115] and experimental realization.[17,71,73–77,82,104] The compositional and architectural complexity of multiblock polymers grows rapidly with the number of blocks and number of monomer chemistries, which has been referred to as a possible Pandora's box[1] because it makes systematic exploration of the phase diagrams infeasible experimentally and, most often, computationally as well. Even the case of an ABC triblock terpolymer involves three χ_{ij} parameters, two conformational asymmetry parameters, and two volume fractions, and this system is known to produce a large array of different morphologies.[141,142] A similar level of combinatorial complexity is introduced by blending, along with the additional challenge of macroscopic phase separation in the multicomponent mixture.

Although the additional complexity is a possible Pandora's box, it also may offer a panacea for the design of increasingly complex nanostructures.[1] In the context of Frank-Kasper phases, the balance between the Pandora's box challenge of increasing complexity is far outweighed by its potential to increase both the stability windows and the number of Frank-Kasper phases produced by block polymers. We have already seen evidence in support of this claim, with the first stable Laves phases appearing in homopolymer/block polymer blends[73,106,107] and the importance of the SIS′O system in experiments.[17,71,82] Comparing blending to multiblock polymers, the blended systems should be the more powerful approach due to the reduced synthetic load; a much wider range of average compositions can be realized by blending versus multiblocks, as illustrated by comparing the diblock blending study of Lindsay *et al.*[76] to the SIS′O multiblock work of Chanpuriya *et al.*[71] From a computational standpoint, a particular challenge here is the potential for missing a possible candidate phase amongst the many possible morphologies possible in complex systems. This is a reason for some caution if one attempts a brute-force exploration of the state space or some type of guided exploration.[143,144] However, if an SCFT calculation can produce a reasonable free energy difference for a new Frank-Kasper phase, say at least $10^{-3}k_{\mathrm{B}}T$ per chain where k_{B} is Boltzmann's constant and T is the absolute temperature,[60] and produces a qualitative explanation underlying the selection of the ordered state, akin to what we saw for diblock polymer blends in Fig. 9, the prediction should provide motivation to pursue it experimentally. Indeed, even if a candidate phase that ultimately proves to be the stable state was missing in the SCFT calculations, its serendipitous emergence in the ensuing experiment would be an interesting result nonetheless.

One salient challenge in computational modeling of systems with more than two monomer types is the accuracy of the underlying parameters, in particular how the χ parameters depend on temperature. Since the Frank-Kasper phases often emerge from a subtle balance between the interfacial tension and chain stretching,[4] and normally have nearly degenerate free energies,[4,60,91] small changes in χ can dramatically affect the phase diagram. Using the

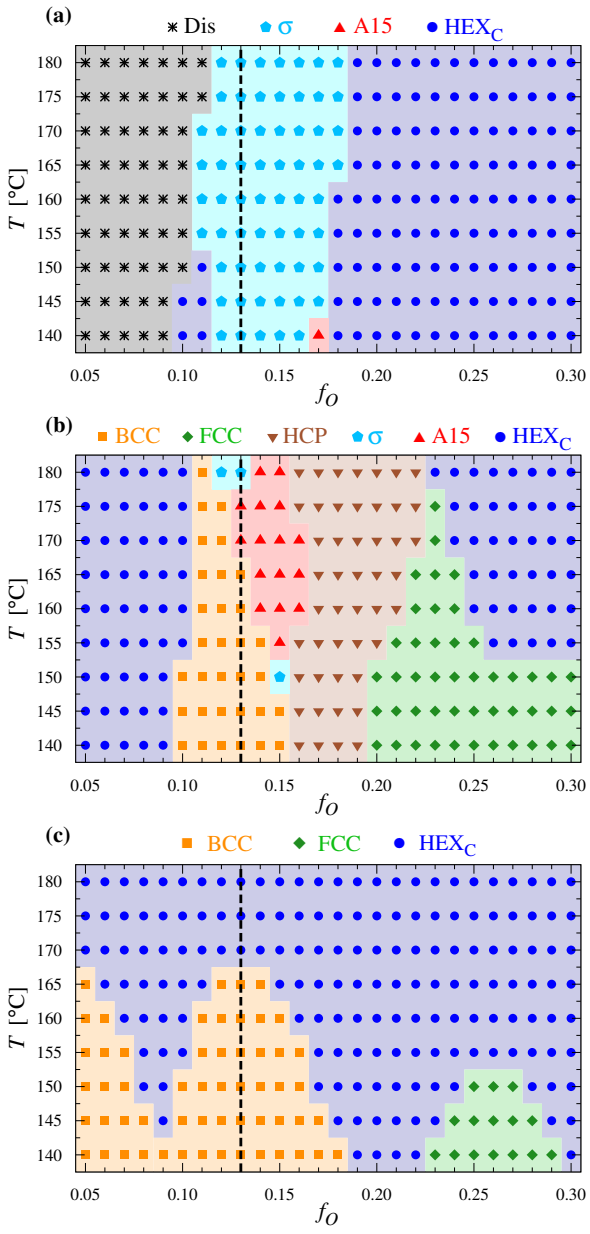

Figure 14: SCFT predictions for an SIS′O tetrablock terpolymer with $\tau = 0.73$, $f_I/(f_S + f_{S'}) = 0.50$ with the O-block added to a parent SIS′ triblock terpolymer with degree of polymerization $N = 298$.[145] (a) χ parameters obtained from the mean-field order-disorder transition. (b) χ parameters obtained from fitting to molecular dynamics simulations. (c) χ parameters obtained from renormalized one-loop theory. Reproduced with permission from Arora, A.; Pillai, N.; Bates, F. S.; Dorfman, K. D. Predicting the phase behavior of ABAC tetrablock terpolymers: Sensitivity to Flory–Huggins interaction parameters. *Polymer* **2018**, *154*, 305–314. Copyright 2018 Elsevier.

SIS′O system as a representative example, Fig. 14 reproduces the results of SCFT calculations using χ parameters obtained by fitting (a) the mean-field order-disorder transition,[146–148] (b)

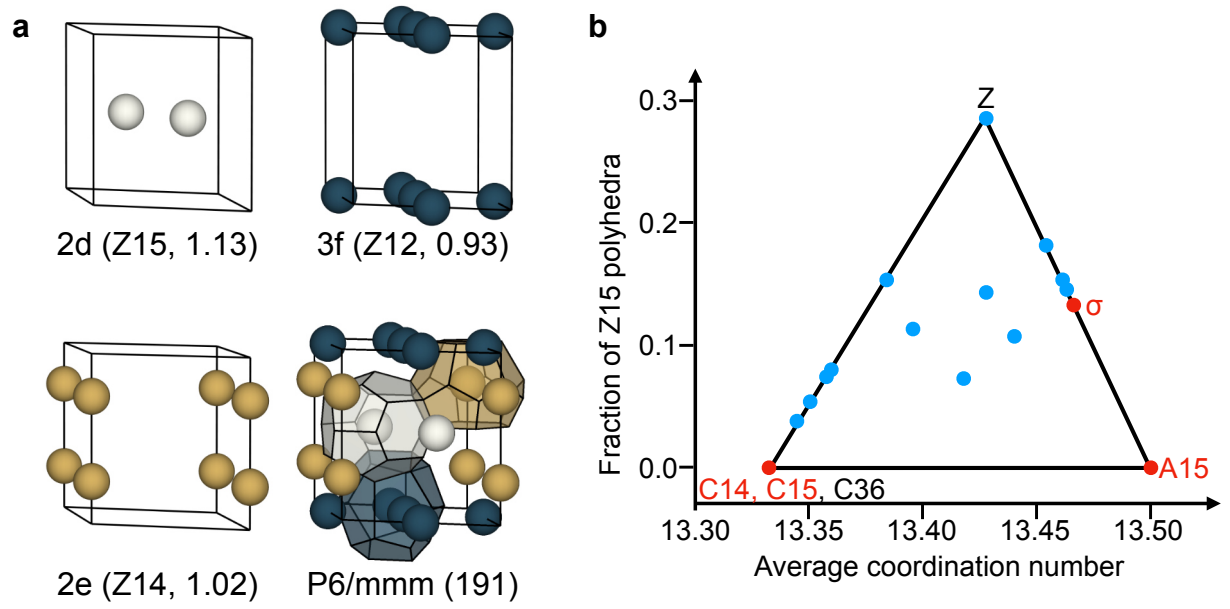

Figure 15: Frank-Kasper Z phase. (a) Structure of the Z phase. The notation is the same as Fig. 2. Coordinates from Ref. 152. Additional information available in the Supporting Information of Ref. 4. (b) Comparison of all known Frank-Kasper phases in terms of the average coordination number and fraction of Z15 polyhedra. The labeled red dots are the Frank-Kasper phases found to date in block polymers. Panel (b) adapted with permission from Su, Z.; Hsu, C.-h.; Gong, Z.; Feng, X.; Huang, J.; Zhang, R.; Wang, Y.; Mao, J.; Wesdemiotis, C.; Li, T.; Seifert, S.; Zhang, W.; Aida, T.; Huang, M.; Cheng, S. Z. D. Identification of a Frank-Kasper Z phase from shape amphiphile self-assembly. *Nat. Chem.* **2019**, *11*, 899–905. Copyright 2019 Springer Nature.

the order-disorder transition from molecular dynamics simulations,[120,140] and (c) renormalized one-loop theory.[149,150] Each of these approaches produced qualitatively different SCFT phase diagrams.[145] Moreover, none of the SCFT predictions for this system[71,110,145] correctly predict the phase sequence with temperature. There is, however, reason for optimism going forward in this vein, owing to a recent breakthrough in the methods for estimating χ parameters from experimental data.[151]

If we are willing to risk opening Pandora's box for this problem, it is important to push the boundaries of the known Frank-Kasper phases in block polymers. A particularly attractive material target is the Z phase illustrated in Fig. 15a. The Z phase is more spherical than σ (number-averaged IQ = 0.7634, see Table S-1), but also possesses more volume asymmetry

than even C14 and C15. Moreover, in contrast to the AB_2 particle stoichiometry that characterizes the Laves phases,[20] the Z phase has three particles of distinctly different volumes. Stabilizing the Z phase thus requires simultaneously achieving high average sphericity and large volume asymmetry. The reason for pursuing Z as the target is illustrated by Figure 15b, which depicts all of the known Frank-Kasper phases in terms of their average coordination number and the fraction of particles with 15-fold coordination.[37] Each of the Frank-Kasper phases can be constructed from linear combinations of the building blocks on the corners of Fig. 15b.[153] Inasmuch as the corners created by A15 and the Laves C14 and C15 have been observed in block polymers, Z remains as the unrealized cornerstone.[154]

There is reason to be optimistic that a Z phase can be realized in a block polymer material. The Z phase was found in a giant shape amphiphile,[37] which demonstrates that there is nothing intrinsic about soft matter that precludes it. A block polymer Z phase cannot emerge from the same mechanism as the giant shape amphiphile;[37,154] the latter system produces the large volume asymmetry through a very low aggregation number of 3 or 4 molecules. However, allowing for blends of different block polymers could stabilize a large volume asymmetry as well if the core blocks of each polymer were also incompatible. The real challenge here does not seem to be finding a Z phase (although its emergence would still be a significant breakthrough), but rather determining the minimum requirements to form Z in a block polymer system. In this respect, it would be very interesting to produce the Z phase in an appropriately designed multiblock polymer, since this would be a single component material. A possible direction here is to combine the macromolecular metallurgy concept,[111] which can generate different particle sizes, with a matrix segregation effect[71] similar to what we saw in Fig. 11 to control the particle-particle interactions to position them onto the Z-phase lattice.

Fluctuation effects and the limits of mean-field theory

Self-consistent field theory has been the workhorse method for the study of Frank-Kasper phase formation in block polymers. There are good reasons for this methodological choice, since the calculations are (relatively) fast compared to coarse-grained molecular dynamic simulations and field theoretic methods, and SCFT provides direct access to the free energy. In most of the cases described so far, SCFT was also used to obtain a qualitative understanding of the mechanisms stabilizing Frank-Kasper phases, including the need for conformational asymmetry,[16,95] the segregation effects in block polymer blends,[103] selective partitioning of homopolymer in block polymer/homopolymer blends,[106,107] matrix segregation effects in multiblock polymers,[71] and the looping and bridging mechanisms in multiblock polymers.[71,110] So long as the goal in using SCFT is to gain these types of qualitative mechanistic insights, it is surely the preferred methodology. For example, the search for the Z phase (and any other target phase) in blends and multiblock polymers, where the parameter space is high dimensional, should be pursued via SCFT, probably in conjunction with an automated searching method.[143,144]

The key issue going forward are accurate predictions of free energies to compare the relative stability of different phases once a promising region of the phase space has been identified via SCFT. This is a subtle point since SCFT is generally regarded as a reasonable predictor of order-order transitions (but qualitatively incorrect near the order-disorder transition). Indeed, direct comparisons of the free energy predicted by SCFT for compositionally asymmetric systems and similar calculations made from well-tempered metadynamics simulations of a calibrated coarse-grained molecular dynamics model generally yield good agreement.[155] If the goal is to predict, say, the bcc-hex transition with increasing f_{A} then the accuracy of SCFT is sufficient because the free energies of these distinctly different phases vary quickly with f_{A} near the order-order transition, even at modest values of $\bar{N}$.

The situation is more challenging for order-order transitions between Frank-Kasper phases. As illustrated in Fig. 2, the Frank-Kasper phases all comprise particles that are organized

differently in space and with somewhat different volumes. There is a free energy difference between these different configurations, but it is small. This issue of near degeneracy of the free energies was known at the outset of the SCFT studies of Frank-Kasper phases, with the seminal calculations reporting a stable A15 phase in multiply branched diblock polymers noting that fcc, bcc and A15 only differed to within 1% throughout the phase diagram.[16] Subsequent work has continued to produce similar degeneracies in other systems.[59,60,91,110] Figure 16a shows one particular example for the σ to A15 transition for a very conformationally asymmetric system $\epsilon = 3$.[59] The free energy differences here are within $10^{-4} k_{\mathrm{B}}T$ per chain. These nearly degenerate free energies are consistent with those reported along with the discovery of the Laves phases, where C14 and C15 are nearly degenerate throughout the entire state space.[60] The diblock foam model also furnished qualitatively similar results over a set of 11 different Frank-Kasper phases, with the free energies the same to within 0.08%.[4]

The near degeneracy of Frank-Kasper phases suggests that fluctuation effects may play an important role for order-order transitions. To date, there is only a single study of these effects,[59] which is reproduced in Fig. 16b. Fluctuations indeed play a critical role in this case, stabilizing A15 relative to σ over the full range of compositions and thus correctly predicting the disorder-to-A15 transition observed in experiments.[59] Importantly, the fully fluctuating calculations produce a relative free energy difference near $10^{-2} k_{\mathrm{B}}T$ per chain, two orders of magnitude larger than that predicted by SCFT in Fig. 16a. Although fluctuation effects may be small compared to other the contributions to the free energy already captured by SCFT,[156] they are sensible relative to the SCFT free energy differences between phases.

Clearly, there is the opportunity to do more with fluctuation effects beyond the pioneering results[59] reproduced in Fig. 16. Since these are expensive calculations, one needs to be judicious in selecting appropriate problems where the cost is worthwhile. We have already alluded to the potential for fluctuation effects to resolve the conformational asymmetry conundrum, and that calculation seems like a reasonable next step for incorporating fluctuations. An arguably more important takeaway message is that SCFT phase diagrams

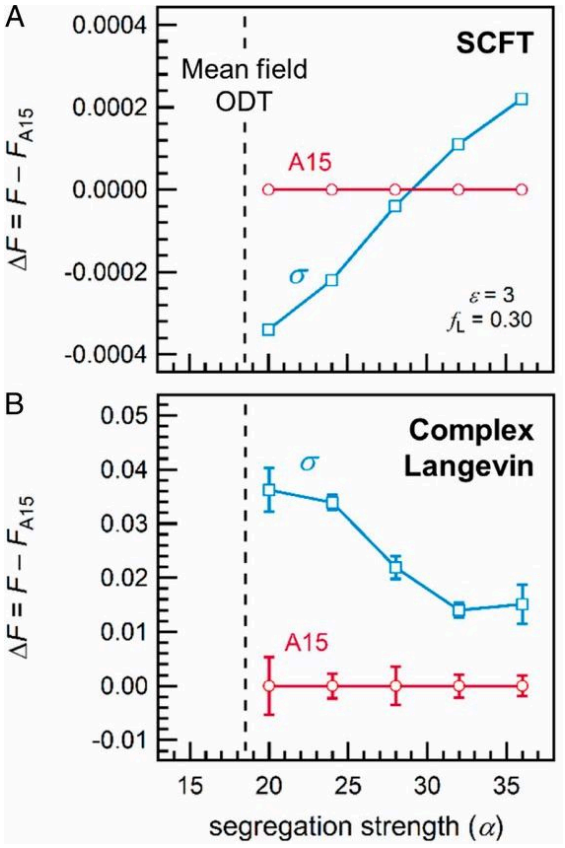

Figure 16: Comparison between (a) SCFT and (b) complex Langevin field theoretic simulations for the relative free energy of A15 and σ.[59] The parameter α is related to χN.[59] Reproduced with permission from Bates, M. W.; Lequieu, J.; Barbon, S. M.; Lewis III, R. M.; Delaney, K. T.; Anastasaki, A.; Hawker, C. J.; Fredrickson, G. H.; Bates, C. M. Stability of the A15 phase in diblock copolymer melts. *Proc. Natl. Acad. Sci. USA* **2019**, *116*, 13194–13199. Copyright 2019 National Academy of Sciences.

for Frank-Kasper phases need to be treated with a certain degree of skepticism, and that the results appearing in those diagrams need to be accompanied by explicit statements of the magnitude of the free energy differences between phases. Likewise, the most promising avenues for SCFT-inspired experiments should be those cases where the prediction of a new phase is accompanied by a qualitative mechanistic basis rather than solely the prediction of a (slightly) lower free energy.

Frank-Kasper phase formation in soft matter

While the primary focus of this Perspective is on Frank-Kasper phase formation in block polymers, these phases have been reported in a variety of other forms of soft matter, often in advance of their discovery in block polymers. For example, both the A15 phase[21] and C15 phase[22,23] were reported in lyotropic liquid crystals three decades ago, and the first σ phase[31] and DDQC[32] were observed in dedrimers almost two decades ago. Other important examples of Frank-Kasper phase discovery in non-polymeric soft matter include the more recent reports of σ[157] and C14 in liquid crystals,[26] as well as work in giant shape amphiphiles[34,35,38] that produced all of the Frank-Kasper phases discussed here and, as noted previously, the first example of a soft matter Z phase.[37]

Given the ubiquity of Frank-Kasper phases across different forms of soft matter, it is worthwhile to consider whether any of the principles underlying their emergence can be translated between different types of soft matter. There are already several exemplary cases of translation. For example, the miktoarm architecture, which was key to establishing the importance of conformational asymmetry in the formation of the σ phase,[95] is an analog of multi-tailed surfactants.[96] Likewise, dendrimeric polymer architectures that mimic their small molecule counterparts[31,32] led to the first prediction of A15[16] and have been predicted by SCFT to provide wide Frank-Kasper phase windows, in particular for A15.[158,159] Similarly, the idea for using core-block homopolymer to produce Laves phases[73] came from previous experiments on particle swelling in oil-water-surfactant mixtures.[26] Looking in the reverse direction, the principle of maximizing particle sphericity to produce σ in block polymers[39] inspired a similar principle of ionic sphericity to explain the σ phase in in ionic surfactants.[157]

One particularly intriguing question of translation is whether electrostatic effects in ionic surfactants, as highlighted by the aforementioned ionic sphericity concept,[26] can be exploited to drive Frank-Kasper phase formation in polymer systems. While it seems unlikely that the ion-specific effects that drive some low-symmetry phases in ionic surfactants[28] will be accessible in polymeric systems, electrostatic effects can be realized using either charged blocks or

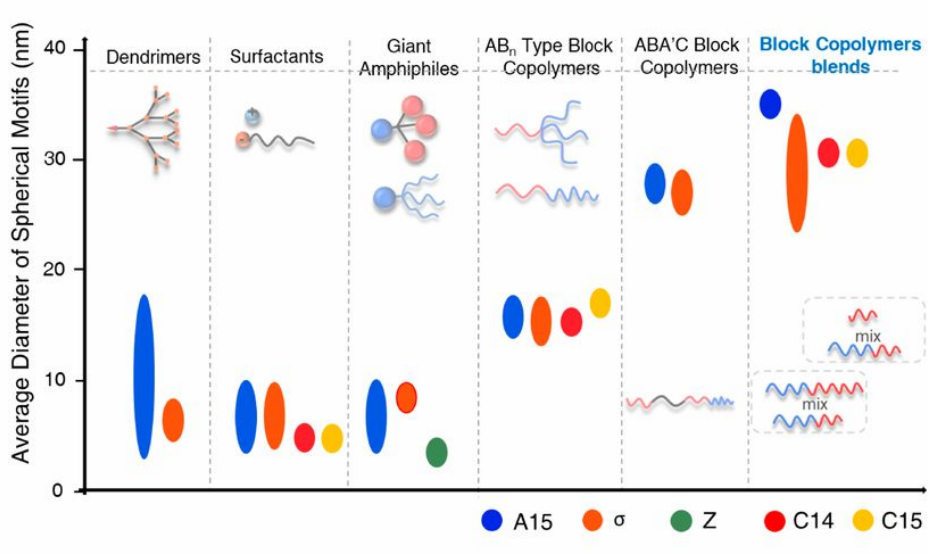

Figure 17: Average particle diameters observed for different Frank-Kasper phases in soft matter. Reproduced with permission from Su, Z.; Huang, M.; Cheng, S. Z. D. Complex self-assembled lattices from simple polymer blends. *Proc. Natl. Acad. Sci. USA* **2020**, *117*, 19618–19620. Copyright 2020 National Academy of Sciences.

blending with ionic liquids. The latter strategy was used to produce a giant C15 phase with a 121 nm unit cell in a blend of poly(styrene)-*b*-poly(ethylene oxide) with homopolymers of both blocks and the ionic liquid LiTFSI.[46] A route to an A15 phase also was reported by first randomly sulfonating the styrene block in a PS-*b*-PMB (PMB = polymethylbutylene) diblock copolymer and then blending the product with the ionic liquid 2E4MIm/HTFSI.[48] From a simulation standpoint, it will be interesting to see whether emerging field theoretic methods for incorporating electrostatic effects[160] will be able to motivate future experiments.

While there are certainly similarities between different forms of soft matter, it is important to recognize their intrinsic differences as well. Figure 17 illustrates the most salient difference between polymers and small molecules — the average size of their micellar particles.[45] The larger particle sizes is both a blessing and a curse for polymer systems. From the standpoint of applications, if one wants to realize potential optical applications of these materials[40–44] into visible wavelengths, the longer length scales accessed by block polymer micelles is a significant benefit. However, these larger length scales are achieved by cor-

respondingly larger aggregation numbers. For example, a typical block polymer melt that forms a Frank-Kasper phase has an aggregation number of hundreds of chains per particle,[60] whereas the corresponding surfactant[157] or dendrimer[31] system has an aggregation number of tens of molecules. Lower aggregation numbers should be connected to the ability to stabilize larger volume asymmetries between particles since the exchange of one chain has a larger effect on the particle volume. Indeed, the giant shape amphiphile system that produced the Z phase had 3 or 4 molecules per particle,[37] which leads to large volume fluctuations due to single molecule exchange. The effect is a digitization of the particle sizes,[154] which can have profound impacts on the phase selection. Indeed, while A15 produces the minimum area Wigner-Seitz cells for equal sized particles,[89] the Z phase becomes the minimum area for a 4:3 volume ratio.[154]

The level of digitization achieved by giant shape amphiphiles[37,154] clearly is inaccessible in polymer systems. However, there is certainly merit to understanding how Frank-Kasper phase formation in block polymers is impacted as $\bar{N}$ decreases; this question has been a persistent theme of this Perspective and is clearly at the forefront of research in this area. There may be some merit to accounting for the finite extensibility of a shorter polymer but staying within the mean-field approximation,[161–163] which has proven useful[164] in modeling the domain spacing in discrete block oligomers[70] and comes at a relatively low computational cost since it is still an SCFT calculation. However, in light of the significant changes in free energy due to fluctuation effects exposed in the analysis of the A15 phase[59] reproduced in Fig. 16, solely correcting for the finite extensibility is unlikely to be sufficient to capture all of the key physics of finite-length polymers.

Frank-Kasper phase formation in metals

The grand challenge in this area is to understand the connections (or lack thereof) between Frank-Kasper phase formation in soft matter, using block polymers as the model system, and the formation of similar phases in metallic alloys. This goal is very ambitious, but there

has been some progress. For example, many low coordination number packings that mimic metallurgy have been predicted in SCFT by tuning the structure of multiblock polymers,[111] and the experimental thermal processing routes[60,63,91] illustrated in Figs. 7-8 have clear analogies to metallurgy. The most notable connection between metals and soft matter in the context of Frank-Kasper phase formation dealt with the principle of sphericity.[39] In their development of the sphericity theory, Lee *et al.*[39] made a remarkably deep connection between their argument for a preference towards high sphericity in real space for soft matter particles, which equilibrate through exchange of mass, and an analogous argument for sphericity in reciprocal space for metals, which equilibrate through exchange of charge. The preference towards higher sphericity of the Wigner-Sietz cells (in block polymers) and the Jones zone (in metals) suggests that these two effects may be related.[39] As pointed out by Lifshitz,[165] perhaps the most interesting potential application of this analogy is to use polymers to provide insights into the formation of 12-fold coordinated quasicrystals in metals and, if we think in the opposite direction, to use the principles that produce 5-fold and 10-fold symmetric quasicrystals in metals to discover the same structures in soft matter.

Concluding remarks

The prediction of an A15 Frank-Kasper phase in 2003[16] and the subsequent discovery of the σ phase in experiments in 2010[17] have led to a renewed interest in understanding the particle-forming region of the block polymer phase diagram. Subsequent work reviewed here has uncovered a number of principles guiding the formation of Frank-Kasper phases in diblock polymers, blends, and multiblock polymers, leading to a qualitative picture of the factors that stabilize Frank-Kasper phases over classical packings such as bcc. However, a comprehensive understanding of the quantitative factors giving rise to Frank-Kasper phases, let alone the exploitation of those principles to discover new phases, remain open questions. The most interesting avenues for future work outlined here are not trivial pursuits; they are

predicated on fluctuation effects, non-equilibrium processing, and the efficient exploration of large design spaces that pose challenges for both experiments and theory. Although these new directions may appear daunting at first glance, the rewards for pursuing them are potentially very high. From a myopic perspective, these research directions would resolve the unanswered questions related to Frank-Kasper phases in block polymers that have been outlined here. Looking more broadly, understanding the roles of fluctuations and processing or discovering new Frank-Kasper phases in block polymers may provide the needed insights required to elucidate the unifying mechanisms (or lack thereof) for Frank-Kasper phase formation across disparate forms of soft matter, or even make a stronger connection between their formation in soft and hard matter. Such a unification, or the demonstration that no such unification exists, would represent a significant intellectual achievement. Block polymer systems have already proven to be a powerful platform for making the first inroads in these directions, and should continue to be a productive model system for many years to come.

Acknowledgement

I thank Frank Bates, Ryan Collanton, Aaron Lindsay, Benjamin Magruder and Mahesh Mahanthappa for discussions that informed some of the content of this manuscript. The code used to create Fig. 2, Fig. 15a and Table S1 as developed by Aaron Lindsay, with input from Andreas Mueller, and is available at https://hdl.handle.net/11299/223279. Their code relies on algorithms and resources in Refs. 166–169. This work was supported by NSF DMR-1719692 and DMR-1725272.

Author Biography

Kevin D. Dorfman is a Distinguished McKnight University Professor in the Department of Chemical Engineering and Materials Science at the University of Minnesota. He received his Ph.D. in Chemical Engineering from MIT in 2002, working with Howard Brenner, and completed postdoctoral research at L'Institut Curie under the supervision of Jean-Louis Viovy prior to joining the University of Minnesota in 2006. His current research interests include simulations of block polymer self-assembly, the properties of DNA in flow and confinement, and printed electronic biosensors.

Supporting Information

Tiling of the σ phase and A15; construction of the Laves phases; Table S-1; additional information on conformational asymmetry

References

(1) Bates, F. S.; Hillmyer, M. A.; Lodge, T. P.; Bates, C. M.; Delaney, K. T.; Fredrickson, G. H. Multiblock Polymers: Panacea or Pandora's Box? *Science* **2012**, *336*, 434–440.

(2) Koizumi, S.; Hasegawa, H.; Hashimoto, T. Ordered structure in blends of block copolymers. 3. Self-assembly in blends of sphere- or cylinder-forming copolymers. *Macromolecules* **1994**, *27*, 4371–4381.

(3) Bates, F. S.; Berney, C. V.; Cohen, R. E. Microphase Structure of Solvent-Cast Diblock Copolymers and Copolymer-Homopolymer Blends Containing Spherical Microdomains. *Macromolecules* **1983**, *16*, 1101–1108.

(4) Reddy, A.; Buckley, M. B.; Arora, A.; Bates, F. S.; Dorfman, K. D.; Grason, G. M. Stable Frank-Kasper phases of self-assembled, soft matter spheres. *Proc. Natl. Acad. Sci. USA* **2018**, *115*, 10233–10238.

(5) Grason, G. M. The packing of soft materials: Molecular asymmetry, geometric frustration and optimal lattices in block copolymer melts. *Phys. Rep.* **2006**, *433*, 1–64.

(6) Leibler, L. Theory of microphase separation in block copolymers. *Macromolecules* **1980**, *13*, 1602–1617.

(7) Pedemonte, E.; Turturro, A.; Bianchi, U.; Devetta, P. The cubic structure of a SIS three block copolymer. *Polymer* **1973**, *14*, 145–150.

(8) Semenov, A. N. Microphase separation in diblock-copolymer melts: Ordering of micelles. *Macromolecules* **1989**, *22*, 2849–2851.

(9) Matsen, M. W.; Bates, F. S. Unifying weak-and strong-segregation block copolymer theories. *Macromolecules* **1996**, *29*, 1091–1098.

(10) Dormidontova, E. E.; Lodge, T. P. The order-disorder transition and the disordered micelle regime in sphere-forming block copolymer melts. *Macromolecules* **2001**, *34*, 9143–9155.

(11) Huang, Y. Y.; Hsu, J. Y.; Chen, H. L.; Hashimoto, T. Existence of fcc-packed spherical micelles in diblock copolymer melt. *Macromolecules* **2007**, *40*, 406–409.

(12) Hsu, N. W.; Nouri, B.; Chen, L. T.; Chen, H. L. Hexagonal Close-Packed Sphere Phase of Conformationally Symmetric Block Copolymer. *Macromolecules* **2020**, *53*, 9665–9675.

(13) Zhang, C.; Vigil, D. L.; Sun, D.; Bates, M. W.; Loman, T.; Murphy, E. A.; Barbon, S. M.; Song, J.-a.; Yu, B.; Fredrickson, G. H.; Whittaker, A. K.; Hawker, C. J.; Bates, C. M. Emergence of Hexagonally Close-Packed Spheres in Linear Block Copolymer Melts. *J. Am. Chem. Soc.* **2021**, *143*, 14106–14114.

(14) Bates, F. S.; Cohen, R. E.; Berney, C. V. Small-Angle Neutron Scattering Determination of Macrolattice Structure in a Polystyrene-Polybutadiene Diblock Copolymer. *Macromolecules* **1982**, *15*, 589–592.

(15) Thomas, E. L.; Kinning, D. J.; Alward, D. B.; Henkee, C. S. Ordered Packing Arrangements of Spherical Micelles of Diblock Copolymers in Two and Three Dimensions. *Macromolecules* **1987**, *20*, 2934–2939.

(16) Grason, G. M.; DiDonna, B. A.; Kamien, R. D. Geometric Theory of Diblock Copolymer Phases. *Phys. Rev. Lett.* **2003**, *91*, 058304.

(17) Lee, S.; Bluemle, M. J.; Bates, F. S. Discovery of a Frank-Kasper σ phase in sphere-forming block copolymer melts. *Science* **2010**, *330*, 349–353.

(18) Dutour Sikirić, M.; Delgado-Friedrichs, O.; Deza, M. Space fullerenes: a computer search for new Frank–Kasper structures. *Acta Crystallogr. Sect. A* **2010**, *66*, 602–615.

(19) Frank, F. C.; Kasper, J. S. Complex alloy structures regarded as sphere packings. I. Definitions and basic principles. *Acta Crystallogr.* **1958**, *11*, 184–190.

(20) Frank, F. C.; Kasper, J. S. Complex alloy structures regarded as sphere packings. II. Analysis and classification of representative structures. *Acta Crystallogr.* **1959**, *12*, 483–499.

(21) Vargas, R.; Mariani, P.; Gulik, A.; Luzzati, V. Cubic phases of lipid-containing systems. The structure of phase Q223 (Space group Pm3n). An X-ray scattering study. *J. Mol. Biol.* **1992**, *225*, 137–145.

(22) Luzzati, V.; Vargas, R.; Gulik, A.; Mariani, P.; Seddon, J. M.; Rivas, E. Lipid Polymorphism: A Correction. The Structure of the Cubic Phase of Extinction Symbol Fd–Consists of Two Types of Disjointed Reverse Micelles Embedded in a Three-Dimensional Hydrocarbon Matrix. *Biochemistry* **1992**, *31*, 279–285.

(23) Seddon, J. M.; Zeb, N.; Templer, R. H.; McElhaney, R. N.; Mannock, D. A. An Fd3m lyotropic cubic phase in a binary glycolipid/water system. *Langmuir* **1996**, *12*, 5250–5253.

(24) Ungar, G.; Zeng, X. Frank–Kasper, quasicrystalline and related phases in liquid crystals. *Soft Matter* **2005**, *1*, 95–106.

(25) Perroni, D. V.; Mahanthappa, M. K. Inverse Pm$\bar{3}$n cubic micellar lyotropic phases from zwitterionic triazolium gemini surfactants. *Soft Matter* **2013**, *9*, 7919–7922.

(26) Baez-Cotto, C. M.; Mahanthappa, M. K. Micellar Mimicry of Intermetallic C14 and C15 Laves Phases by Aqueous Lyotropic Self-Assembly. *ACS Nano* **2018**, *12*, 3226–3234.

(27) Holerca, M. N.; Sahoo, D.; Partridge, B. E.; Peterca, M.; Zeng, X.; Ungar, G.; Percec, V. Dendronized Poly(2-oxazoline) Displays within only Five Monomer Repeat Units Liquid Quasicrystal, A15 and σ Frank-Kasper Phases. *J. Am. Chem. Soc.* **2018**, *140*, 16941–16947.

(28) Jayaraman, A.; Mahanthappa, M. K. Counterion-Dependent Access to Low-Symmetry Lyotropic Sphere Packings of Ionic Surfactant Micelles. *Langmuir* **2018**, *34*, 2290–2301.

(29) Jayaraman, A.; Zhang, D. Y.; Dewing, B. L.; Mahanthappa, M. K. Path-Dependent Preparation of Complex Micelle Packings of a Hydrated Diblock Oligomer. *ACS Cent. Sci.* **2019**, *20*, 619–628.

(30) Jayaraman, A.; Baez-Cotto, C. M.; Mann, T. J.; Mahanthappa, M. K. Dodecagonal quasicrystals of oil-swollen ionic surfactant micelles. *Proc. Natl. Acad. Sci. USA* **2021**, *118*, e2101598118.

(31) Ungar, G.; Liu, Y.; Zeng, X.; Percec, V.; Cho, W.-D. Giant supramolecular liquid crystal lattice. *Science* **2003**, *299*, 1208–1211.

(32) Zeng, X.; Ungar, G.; Liu, Y.; Percec, V.; Dulcey, A. E.; Hobbs, J. K. Supramolecular dendritic liquid quasicrystals. *Nature* **2004**, *428*, 157–160.

(33) Lachmayr, K. K.; Wentz, C. M.; Sita, L. R. An Exceptionally Stable and Scalable Sugar–Polyolefin Frank–Kasper A15 Phase. *Angew. Chem. Intl. Ed.* **2020**, *59*, 1521–1526.

(34) Huang, M.; Hsu, C.-H.; Wang, J.; Mei, S.; Dong, X.; Li, Y.; Li, M.; Liu, H.; Zhang, W.; Aida, T.; Zhang, W.-B.; Yue, K.; Cheng, S. Z. D. Selective assemblies of giant tetrahedra via precisely controlled positional interactions. *Science* **2015**, *348*, 424–428.

(35) Yue, K.; Huang, M.; Marson, R. L.; He, J.; Huang, J.; Zhou, Z.; Wang, J.; Liu, C.; Yan, X.; Wu, K.; Guo, Z.; Liu, H.; Zhang, W. B.; Ni, P.; Wesdemiotis, C.; Zhang, W. B.; Glotzer, S. C.; Cheng, S. Z. D. Geometry induced sequence of nanoscale Frank-Kasper and quasicrystal mesophases in giant surfactants. *Proc. Natl. Acad. Sci. USA* **2016**, *113*, 14195–14200.

(36) Huang, M.; Yue, K.; Wang, J.; Hsu, C. H.; Wang, L.; Cheng, S. Z. D. Frank-Kasper and related quasicrystal spherical phases in macromolecules. *Science China Chem.* **2018**, *61*, 33–45.

(37) Su, Z.; Hsu, C.-h.; Gong, Z.; Feng, X.; Huang, J.; Zhang, R.; Wang, Y.; Mao, J.; Wesdemiotis, C.; Li, T.; Seifert, S.; Zhang, W.; Aida, T.; Huang, M.; Cheng, S. Z. D. Identification of a Frank-Kasper Z phase from shape amphiphile self-assembly. *Nat. Chem.* **2019**, *11*, 899–905.

(38) Liu, Y.; Liu, T.; Yan, X.-y.; Guo, Q.-Y.; Wang, J.; Zhang, R.; Zhang, S.; Su, Z.; Huang, J.; Liu, G.-x.; Zhang, W.; Zhang, W.; Aida, T.; Yue, K.; Huang, M.; Cheng, S. Z. D. Mesoatom Alloys via Self-sorting Approach of Giant Molecules Blends. *Giant* **2020**, *4*, 100031.

(39) Lee, S.; Leighton, C.; Bates, F. S. Sphericity and symmetry breaking in the formation of Frank–Kasper phases from one component materials. *Proc. Natl. Acad. Sci. USA* **2014**, *111*, 17723–17731.

(40) Man, W.; Megens, M.; Steinhardt, P. J.; Chaikin, P. M. Experimental measurement of the photonic properties of icosahedral quasicrystals. *Nature* **2005**, *436*, 993–996.

(41) Hynninen, A.-P.; Thijssen, J. H. J.; Vermolen, E. C. M.; Dijkstra, M.; van Blaaderen, A. Self-assembly route for photonic crystals with a bandgap in the visible region. *Nat. Mater.* **2007**, *6*, 202–205.

(42) Rechtsman, M. C.; Jeong, H. C.; Chaikin, P. M.; Torquato, S.; Steinhardt, P. J. Optimized structures for photonic quasicrystals. *Phys. Rev. Lett.* **2008**, *101*, 073902.

(43) Florescu, M.; Torquato, S.; Steinhardt, P. J. Complete band gaps in two-dimensional photonic quasicrystals. *Phys. Rev. B* **2009**, *80*, 155112.

(44) Klatt, M. A.; Steinhardt, P. J.; Torquato, S. Phoamtonic designs yield sizeable 3D photonic band gaps. *Proc. Natl. Acad. Sci. USA* **2019**, *116*, 23480–23486.

(45) Su, Z.; Huang, M.; Cheng, S. Z. D. Complex self-assembled lattices from simple polymer blends. *Proc. Natl. Acad. Sci. USA* **2020**, *117*, 19618–19620.

(46) Xie, S.; Lindsay, A. P.; Bates, F. S.; Lodge, T. P. Formation of a C15 Laves Phase with a Giant Unit Cell in Salt-Doped A/B/AB Ternary Polymer Blends. *ACS Nano* **2020**, *14*, 13754–13764.

(47) Joannopoulos, J. D.; Villeneuve, P. R.; Fan, S. Photonic crystals: putting a new twist on light. *Nature* **1997**, *386*, 143–149.

(48) Min, J.; Jun, H. Y.; Jeong, S.; Lee, B.; Son, C. Y.; Park, M. J. Enhancing ion transport in charged block copolymers by stabilizing low symmetry morphology: Electrostatic control of interfaces. *Proc. Natl. Acad. Sci. USA* **2021**, *118*, e2107987118.

(49) Matsen, M. W. The standard Gaussian model for block copolymer melts. *J. Phys. Condens. Matter* **2002**, *14*, 21–47.

(50) Ceniceros, H. D.; Fredrickson, G. H. Numerical Solution of Polymer Self-Consistent Field Theory. *Multiscale Model. Simul.* **2004**, *2*, 452–474.

(51) Fredrickson, G. H. *The equilibrium theory of inhomogeneous polymers*; Oxford University Press: Oxford, 2006.

(52) Arora, A.; Qin, J.; Morse, D. C.; Delaney, K. T.; Fredrickson,G. H.; Bates, F. S.; Dorfman, K. D. Broadly Accessible SCFT for Block Polymer Materials Discovery. *Macromolecules* **2016**, *49*, 4675–4690.

(53) Shi, A. C. Self-Consistent Field Theory of Inhomogeneous Polymeric Systems. In *Variational Methods in Molecular Modeling*; Wu, J., Ed.; Springer: Singapore, 2017; pp 155–180.

(54) Stein, F.; Leineweber, A. Laves phases: a review of their functional and structural applications and an improved fundamental understanding of stability and properties. *J. Mater. Sci.* **2020**, *56*, 5321–5427.

(55) Bergman, G.; Shoemaker, D. P. The determination of the crystal structure of the σ phase in the iron–chromium and iron–molybdenum systems. *Acta Crystallogr.* **1954**, *7*, 857–865.

(56) Lawson, A. C.; Olsen, C. E.; Richardson, J. W.; Mueller, M. H.; Lander, G. H. Structure of β-Uranium. *Acta Crystallogr. Sect. B* **1988**, *44*, 89–96.

(57) Arakcheeva, A.; Chapuis, G.; Birkedal, H.; Pattison, P.; Grinevitch, V. The commensurate composite σ-structure of β-tantalum. *Acta Crystallogr. Sect. B* **2003**, *59*, 324–336.

(58) Graef, M. D.; McHenry, M. E. *Structure of materials*; Cambridge University Press, 2012.

(59) Bates, M. W.; Lequieu, J.; Barbon, S. M.; Lewis III, R. M.; Delaney, K. T.; Anastasaki, A.; Hawker, C. J.; Fredrickson, G. H.; Bates, C. M. Stability of the A15 phase in diblock copolymer melts. *Proc. Natl. Acad. Sci. USA* **2019**, *116*, 13194–13199.

(60) Kim, K.; Schulze, M. W.; Arora, A.; Lewis III, R. M.; Hillmyer, A.; Dorfman, K. D.; Bates, F. S. Thermal Processing of Diblock Copolymer Melts Mimics Metallurgy. *Science* **2017**, *356*, 520–523.

(61) Uddin, M. H.; Rodriguez, C.; López-Quintela, A.; Leisner, D.; Solans, C.; Esquena, J.; Kunieda, H. Phase behavior and microstructure of poly(oxyethylene)-poly(dimethylsiloxane) copolymer melt. *Macromolecules* **2003**, *36*, 1261–1271.

(62) Aroyo, M. I.; Perez-Mato, J. M.; Capillas, C.; Kroumova, E.; Ivantchev, S.; Madariaga, G.; Kirov, A.; Wondratschek, H. Bilbao Crystallographic Server: I. Databases and crystallographic computing programs. *Zeitschrift fur Krist.* **2006**, *221*, 15–27.

(63) Gillard, T. M.; Lee, S.; Bates, F. S. Dodecagonal quasicrystalline order in a diblock copolymer melt. *Proc. Natl. Acad. Sci. USA* **2016**, *113*, 5167–5172.

(64) Schulze, M. W.; Lewis III, R. M.; Lettow, J. H.; Hickey, R. J.; Gillard, T. M.; Hillmyer, M. A.; Bates, F. S. Conformational Asymmetry and Quasicrystal Approximants in Linear Diblock Copolymers. *Phys. Rev. Lett.* **2017**, *118*, 207801.

(65) Jeon, S.; Jun, T.; Jo, S.; Ahn, H.; Lee, S.; Lee, B.; Ryu, D. Y. Frank–Kasper Phases Identified in PDMS-b-PTFEA Copolymers with High Conformational Asymmetry. *Macromol. Rapid Commun.* **2019**, *40*, 1900259.

(66) Barbon, S. M.; Song, J.-a.; Chen, D.; Zhang, C.; Lequieu, J.; Delaney, K. T.; Anastasaki, A.; Rolland, M.; Fredrickson, G. H.; Bates, M. W.; Hawker, C. J.; Bates, C. M. Architecture Effects in Complex Spherical Assemblies of $(AB)_n$-Type Block Copolymers. *ACS Macro Lett.* **2020**, *9*, 1745–1752.

(67) Mueller, A. J.; Lindsay, A. P.; Jayaraman, A.; Lodge, T. P.; Mahanthappa, M. K.; Bates, F. S. Quasicrystals and Their Approximants in a Crystalline-Amorphous Diblock Copolymer. *Macromolecules* **2021**, *54*, 2647–2660.

(68) Lindsay, A. P.; Jayaraman, A.; Peterson, A. J.; Mueller, A. J.; Weigand, S.; Mahanthappa, M. K.; Lodge, T. P.; Bates, F. S. Reevaluation of Poly(ethylene-alt-propylene)-block-Polydimethylsiloxane Phase Behavior Uncovers Topological Close-Packing and Epitaxial Quasicrystal Growth. *ACS Nano* **2021**, *15*, 9453–9468.

(69) Bates, M. W.; Barbon, S. M.; Levi, A. E.; Lewis III, R. M.; Beech, H. K.; Vonk, K. M.; Zhang, C.; Fredrickson, G. H.; Hawker, C. J.; Bates, C. M. Synthesis and Self-Assembly of AB_n miktoarm star polymers. *ACS Macro Lett.* **2020**, *9*, 396–403.

(70) Sun, Y.; Tan, R.; Gan, Z.; Li, G.; Zhou, D.; Shao, Y.; Zhang, W.-B.; Zhang, R.; Dong, X.-H. Discrete Block Copolymers with Diverse Architectures: Resolving Com-

plex Spherical Phases with One Monomer Resolution. *ACS Cent. Sci.* **2020**, *6*, 1386–1393.

(71) Chanpuriya, S.; Kim, K.; Zhang, J.; Lee, S.; Arora, A.; Dorfman, K. D.; Delaney, K. T.; Fredrickson, G. H.; Bates, F. S. Cornucopia of Nanoscale Ordered Phases in Sphere-Forming Tetrablock Terpolymers. *ACS Nano* **2016**, *10*, 4961–4972.

(72) Chang, A. B.; Bates, F. S. Impact of Architectural Asymmetry on Frank-Kasper Phase Formation in Block Polymer Melts. *ACS Nano* **2020**, *14*, 11463–11472.

(73) Mueller, A. J.; Lindsay, A. P.; Jayaraman, A.; Lodge, T. P.; Mahanthappa, M. K.; Bates, F. S. Emergence of a C15 Laves Phase in Diblock Polymer/Homopolymer Blends. *ACS Macro Lett.* **2020**, *9*, 576–582.

(74) Takagi, H.; Hashimoto, R.; Igarashi, N.; Kishimoto, S.; Yamamoto, K. Frank–Kasper σ phase in polybutadiene-poly(ϵ-caprolactone) diblock copolymer/polybutadiene blends. *J. Phys.: Condens. Matter* **2017**, *29*, 0204002.

(75) Takagi, H.; Hashimoto, R.; Igarashi, N.; Kishimoto, S.; Yamamoto, K. Synchrotron SAXS Studies on Lattice Structure of Spherical Micelles in Binary Mixtures of Block Copolymers and Homopolymers. *J. Fiber Sci. Technol.* **2018**, *74*, 10–16.

(76) Lindsay, A. P.; Lewis III, R. M.; Lee, B.; Peterson, A. J.; Lodge, T. P.; Bates, F. S. A15, σ, and a Quasicrystal: Access to Complex Particle Packings via Bidisperse Diblock Copolymer Blends. *ACS Macro Lett.* **2020**, *9*, 197–203.

(77) Yamamoto, K.; Takagi, H. Frank-Kasper and A-15 phases formed in symmetry and asymmetry block copolymer blend system. *Mater. Trans.* **2021**, *62*, 325–328.

(78) Lindsay, A. P.; Cheong, G. K.; Peterson, A. J.; Weigand, S.; Dorfman, K. D.; Lodge, T. P.; Bates, F. S. Complex phase formation in particle-forming AB/AB′ di-

block copolymer blends with variable core block lengths. *Macromolecules* **2021**, *54*, 7088–7101.

(79) Papadakis, C. M.; Almdal, K.; Mortensen, K.; Vigild, M. E.; Štěánek, P. Unexpected phase behavior of an asymmetric diblock copolymer. *J. Chem. Phys.* **1999**, *111*, 4319–4326.

(80) Talapin, D. V.; Shevchenko, E. V.; Bodnarchuk, M. I.; Ye, X.; Chen, J.; Murray, C. B. Quasicrystalline order in self-assembled binary nanoparticle superlattices. *Nature* **2009**, *461*, 964–967.

(81) Xiao, C.; Fujita, N.; Miyasaka, K.; Sakamoto, Y.; Terasaki, O. Dodecagonal tiling in mesoporous silica. *Nature* **2012**, *487*, 349–353.

(82) Zhang, J.; Bates, F. S. Dodecagonal Quasicrystalline Morphology in a Poly(styrene-b-isoprene-b-styrene-b-ethylene oxide) Tetrablock Terpolymer. *J. Am. Chem. Soc.* **2012**, *134*, 7636–7639.

(83) Takano, A.; Kawashima, W.; Noro, A.; Isono, Y.; Tanaka, N.; Dotera, T.; Matsushita, Y. A mesoscopic Archimedean tiling having a new complexity in an ABC star polymer. *J. Polym. Sci. Part B Polym. Phys.* **2005**, *43*, 2427–2432.

(84) Miyamori, Y.; Suzuki, J.; Takano, A.; Matsushita, Y. Periodic and Aperiodic Tiling Patterns from a Tetrablock Terpolymer System of the A_1BA_2C Type. *ACS Macro Lett.* **2020**, *9*, 32–37.

(85) Ding, Y.; Gadelrab, K. R.; Mizrahi Rodriguez, K.; Huang, H.; Ross, C. A.; Alexander-Katz, A. Emergent symmetries in block copolymer epitaxy. *Nat. Commun.* **2019**, *10*, 2974.

(86) Hayashida, K.; Dotera, T.; Takano, A.; Matsushita, Y. Polymeric quasicrystal: Mesoscopic quasicrystalline tiling in ABC star polymers. *Phys. Rev. Lett.* **2007**, *98*, 1–4.

(87) Duan, C.; Zhao, M.; Qiang, Y.; Chen, L.; Li, W.; Qiu, F.; Shi, A.-C. Stability of Two-Dimensional Dodecagonal Quasicrystalline Phase of Block Copolymers. *Macromolecules* **2018**, *51*, 7713–7721.

(88) Ziherl, P.; Kamien, R. D. Soap froths and crystal structures. *Phys. Rev. Lett.* **2000**, *85*, 3528–3531.

(89) Weaire, D.; Phelan, R. A counter-example to Kelvin's conjecture on minimal surfaces. *Philos. Mag. Lett.* **2004**, *69*, 107–110.

(90) Watanabe, M.; Asai, Y.; Suzuki, J.; Takano, A.; Matsushita, Y. Frank-Kasper A15 Phase Formed in AB_n block-graft copolymers with large numbers of graft chains. *Macromolecules* **2020**, *53*, 10217–10224.

(91) Kim, K.; Arora, A.; Lewis, R. M.; Liu, M.; Li, W.; Shi, A.-C.; Dorfman, K. D.; Bates, F. S. Origins of low-symmetry phases in asymmetric diblock copolymer melts. *Proc. Natl. Acad. Sci. USA* **2018**, *115*, 847–854.

(92) Olmsted, P. D.; Milner, S. T. Strong-segregation theory of bicontinuous phases in block copolymers. *Phys. Rev. Lett.* **1994**, *72*, 936–939.

(93) Olmsted, P. D.; Milner, S. T. Strong-segregation theory of bicontinuous phases in block copolymers. *Macromolecules* **1998**, *31*, 4011–4022.

(94) Bates, F. S.; Schulz, M. F.; Rosedale, J. H.; Almdal, K. Correlation of binary polyolefin phase behavior with statistical segment length. *Macromolecules* **1992**, *25*, 5547–5550.

(95) Xie, N.; Li, W.; Qiu, F.; Shi, A.-C. σ phase formed in conformationally asymmetric AB-type block copolymers. *ACS Macro Lett.* **2014**, *3*, 906–910.

(96) Milner, S. T. Chain Architecture and Asymmetry in Copolymer Microphases. *Macromolecules* **1994**, *27*, 2333–2335.

(97) Bates, F. S.; Fredrickson, G. H. Conformational asymmetry and polymer-polymer thermodynamics. *Macromolecules* **1994**, *27*, 1065–1067.

(98) Li, W.; Liu, Y.-X. Simplicity in mean-field phase behavior of two-component miktoarm star copolymers. *J. Chem. Phys.* **2021**, *154*, 014903.

(99) Bates, F. S.; Schulz, M. F.; Khandpur, A. K.; Förster, S.; Rosedale, J. H.; Almdal, K.; Mortensen, K. Fluctuations, conformational asymmetry and block copolymer phase behaviour. *Faraday Discuss.* **1994**, *98*, 7–18.

(100) Matsen, M. W.; Bates, F. S. Conformationally Asymmetric Block Copolymers. *J. Polym. Sci. Part B Polym. Phys.* **1997**, *35*, 945–952.

(101) Roth, J.; Denton, A. R. Solid-phase structures of the Dzugutov pair potential. *Phys. Rev. E* **2000**, *61*, 6845–6857.

(102) Keys, A. S.; Glotzer, S. C. How do quasicrystals grow? *Phys. Rev. Lett.* **2007**, *99*, 235503.

(103) Liu, M.; Qiang, Y.; Li, W.; Qiu, F.; Shi, A.-C. Stabilizing the Frank-Kasper phases via binary blends of AB diblock copolymers. *ACS Macro Lett.* **2016**, *5*, 1167–1171.

(104) Takagi, H.; Yamamoto, K. Phase Boundary of Frank-Kasper σ Phase in Phase Diagrams of Binary Mixtures of Block Copolymers and Homopolymers. *Macromolecules* **2019**, *52*, 2007–2014.

(105) Zhao, M.; Li, W. Laves Phases Formed in the Binary Blend of AB_4 Miktoarm Star Copolymer and A-Homopolymer. *Macromolecules* **2019**, *52*, 1832–1842.

(106) Cheong, G. K.; Bates, F. S.; Dorfman, K. D. Symmetry breaking in particle-forming diblock polymer/homopolymer blends. *Proc. Natl. Acad. Sci. USA* **2020**, *117*, 16764–16769.

(107) Xie, J.; Shi, A.-C. Formation of complex spherical packing phases in diblock copolymer/homopolymer blends. *Giant* **2021**, *5*, 100043.

(108) Matsen, M. W. Phase Behavior of Block Copolymer/Homopolymer Blends. *Macromolecules* **1995**, *28*, 5765–5773.

(109) Semenov, A. N. Phase equilibria in block copolymer-homopolymer mixtures. *Macromolecules* **1993**, *26*, 2273–2281.

(110) Liu, M.; Li, W.; Qiu, F.; Shi, A.-C. Stability of the Frank-Kasper σ-Phase in BABC Linear Tetrablock Terpolymers. *Soft Matter* **2016**, *12*, 6412–6421.

(111) Xie, N.; Liu, M.; Deng, H.; Li, W.; Qiu, F.; Shi, A.-C. Macromolecular metallurgy of binary mesocrystals via designed multiblock terpolymers. *J. Am. Chem. Soc.* **2014**, *136*, 2974–2977.

(112) Liu, H. H.; Huang, C. I.; Shi, A.-C. Self-Assembly of Linear ABCBA Pentablock Terpolymers. *Macromolecules* **2015**, *48*, 6214–6223.

(113) Chen, L.; Qiang, Y.; Li, W. Tuning Arm Architecture Leads to Unusual Phase Behaviors in a $(BAB)_5$ Star Copolymer Melt. *Macromolecules* **2018**, *51*, 9890–9900.

(114) Dong, Q.; Li, W. Effect of Molecular Asymmetry on the Formation of Asymmetric Nanostructures in ABC-Type Block Copolymers. *Macromolecules* **2021**, *54*, 203–213.

(115) Zhao, B.; Wang, C.; Chen, Y.; Liu, M. Frank-Kasper phases self-assembled from linear $A_1B_1A_2B_2$ tetrablock copolymer. *Langmuir* **2021**, *37*, 5642–5650.

(116) Li, W.; Duan, C.; Shi, A.-C. Nonclassical Spherical Packing Phases Self-Assembled from AB-Type Block Copolymers. *ACS Macro Lett.* **2017**, *6*, 1257–1262.

(117) Fredrickson, G. H.; Helfand, E. Fluctuation effects in the theory of microphase separation in block copolymers. *J. Chem. Phys.* **1987**, *87*, 697–705.

(118) Khandpur, A. K.; Förster, S.; Bates, F. S.; Hamley, I. W.; Ryan, A. J.; Bras, W.; Almdal, K.; Mortensen, K. Polyisoprene-Polystyrene Diblock Copolymer Phase Diagram near the Order-Disorder Transition. *Macromolecules* **1995**, *28*, 8796–8806.

(119) Lewis III, R. M.; Arora, A.; Beech, H. K.; Lee, B.; Lindsay, A. P.; Lodge, T. P.; Dorfman, K. D.; Bates, F. S. Role of Chain Length in the Formation of Frank-Kasper Phases in Diblock Copolymers. *Phys. Rev. Lett.* **2018**, *121*, 208002.

(120) Glaser, J.; Medapuram, P.; Beardsley, T. M.; Matsen, M. W.; Morse, D. C. Universality of block copolymer melts. *Phys. Rev. Lett.* **2014**, *113*, 068302.

(121) Qin, J.; Morse, D. C. Fluctuations in symmetric diblock copolymers: Testing theories old and new. *Phys. Rev. Lett.* **2012**, *108*, 11–14.

(122) Ghasimakbari, T.; Morse, D. C. Correlations in Disordered Melts of Asymmetric Diblock Copolymers. *Macromolecules* **2018**, *51*, 2335–2348.

(123) Fredrickson, G. H.; Ganesan, V.; Drolet, F. Field-theoretic computer simulation methods for polymers and complex fluids. *Macromolecules* **2002**, *35*, 16–39.

(124) Delaney, K. T.; Fredrickson, G. H. Polymer field-theory simulations on graphics processing units. *Comput. Phys. Commun.* **2013**, *184*, 2102–2110.

(125) Düchs, D.; Delaney, K. T.; Fredrickson, G. H. A multi-species exchange model for fully fluctuating polymer field theory simulations. *J. Chem. Phys.* **2014**, *141*, 174103.

(126) Delaney, K. T.; Fredrickson, G. H. Recent Developments in Fully Fluctuating Field-Theoretic Simulations of Polymer Melts and Solutions. *J. Phys. Chem. B* **2016**, *120*, 7615–7634.

(127) Stasiak, P.; Matsen, M. W. Monte Carlo field-theoretic simulations for melts of symmetric diblock copolymer. *Macromolecules* **2013**, *46*, 8037–8045.

(128) Vorselaars, B.; Stasiak, P.; Matsen, M. W. Field-Theoretic Simulation of Block Copolymers at Experimentally Relevant Molecular Weights. *Macromolecules* **2015**, *48*, 9071–9080.

(129) Fredrickson, G. H.; Delaney, K. T. Field-theoretic simulations: An emerging tool for probing soft material assembly. *MRS Bull.* **2018**, *43*, 371–378.

(130) Beardsley, T. M.; Spencer, R. K. W.; Matsen, M. W. Computationally Efficient Field-Theoretic Simulations for Block Copolymer Melts. *Macromolecules* **2019**, *52*, 8840–8848.

(131) Matsen, M. W. Field theoretic approach for block polymer melts: SCFT and FTS. *J. Chem. Phys.* **2020**, *152*, 110901.

(132) Beardsley, T. M.; Matsen, M. W. Fluctuation correction for the order–disorder transition of diblock copolymer melts. *J. Chem. Phys.* **2021**, *154*, 124902.

(133) Miyake, G. M.; Piunova, V. A.; Weitekamp, R. A.; Grubbs, R. H. Precisely tunable photonic crystals from rapidly self-assembling brush block copolymer blends. *Angew. Chem. Intl. Ed.* **2012**, *51*, 11246–11248.

(134) Sveinbjörnsson, B. R.; Weitekamp, R. A.; Miyake, G. M.; Xia, Y.; Atwater, H. A.; Grubbs, R. H. Rapid self-assembly of brush block copolymers to photonic crystals. *Proc. Natl. Acad. Sci. USA* **2012**, *109*, 14332–14336.

(135) Macfarlane, R. J.; Kim, B.; Lee, B.; Weitekamp, R. A.; Bates, C. M.; Lee, S. F.; Chang, A. B.; Delaney, K. T.; Fredrickson, G. H.; Atwater, H. A.; Grubbs, R. H. Improving brush polymer infrared one-dimensional photonic crystals via linear polymer additives. *J. Am. Chem. Soc.* **2014**, *136*, 17374–17377.

(136) Liberman-Martin, A. L.; Chu, C. K.; Grubbs, R. H. Application of Bottlebrush Block Copolymers as Photonic Crystals. *Macromol. Rapid Commun.* **2017**, *38*, 1–15.

(137) Müller, M.; de Pablo, J. J. Computational Approaches for the Dynamics of Structure Formation in Self-Assembling Polymeric Materials. *Annu. Rev. Mater. Res.* **2013**, *43*, 1–34.

(138) Müller, M. Process-directed self-assembly of copolymers: Results of and challenges for simulation studies. *Prog. Polym. Sci.* **2020**, *101*, 101198.

(139) Glaser, J.; Qin, J.; Medapuram, P.; Morse, D. C. Collective and single-chain correlations in disordered melts of symmetric diblock copolymers: Quantitative comparison of simulations and theory. *Macromolecules* **2014**, *47*, 851–869.

(140) Medapuram, P.; Glaser, J.; Morse, D. C. Universal phenomenology of symmetric diblock copolymers near the order-disorder transition. *Macromolecules* **2015**, *48*, 819–839.

(141) Meuler, A. J.; Hillmyer, M. A.; Bates, F. S. Ordered network mesostructures in block polymer materials. *Macromolecules* **2009**, *42*, 7221–7250.

(142) Xu, W.; Jiang, K.; Zhang, P.; Shi, A.-C. A strategy to explore stable and metastable ordered phases of block copolymers. *J. Phys. Chem. B* **2013**, *117*, 5296–5305.

(143) Khadilkar, M. R.; Paradiso, S.; Delaney, K. T.; Fredrickson, G. H. Inverse Design of Bulk Morphologies in Multiblock Polymers Using Particle Swarm Optimization. *Macromolecules* **2017**, *50*, 6702–6709.

(144) Zhao, S.; Cai, T.; Zhang, L.; Li, W.; Lin, J. Autonomous Construction of Phase Diagrams of Block Copolymers by Theory-Assisted Active Machine Learning. *ACS Macro Lett.* **2021**, 1–5.

(145) Arora, A.; Pillai, N.; Bates, F. S.; Dorfman, K. D. Predicting the phase behavior of ABAC tetrablock terpolymers: Sensitivity to Flory–Huggins interaction parameters. *Polymer* **2018**, *154*, 305–314.

(146) Frielinghaus, H.; Hermsdorf, N.; Sigel, R.; Almdal, K.; Mortensen, K.; Hamley, I. W.; Messé, L.; Corvazier, L.; Ryan, A. J.; Van Dusschoten, D.; Wilhelm, M.; Floudas, G.; Fytas, G. Blends of AB/BC diblock copolymers with a large interaction parameter γ. *Macromolecules* **2001**, *34*, 4907–4916.

(147) Frielinghaus, H.; Pedersen, W. B.; Larsen, P. S.; Almdal, K.; Mortensen, K. End Effects in Poly(styrene)/Poly(ethylene oxide) Copolymers. *Macromolecules* **2001**, *34*, 1096–1104.

(148) Frielinghaus, H.; Hermsdorf, N.; Almdal, K.; Mortensen, K.; Messé, L.; Corvazier, L.; Fairclough, J. P.; Ryan, A. J.; Olmsted, P. D.; Hamley, I. W. Micro- vs. macrophase separation in binary blends of poly(styrene)-poly(isoprene) and poly(isoprene)-poly(ethylene oxide) diblock copolymers. *Europhys. Lett.* **2001**, *53*, 680–686.

(149) Qin, J.; Grzywacz, P.; Morse, D. C. Renormalized one-loop theory of correlations in disordered diblock copolymers. *J. Chem. Phys.* **2011**, *135*, 084902.

(150) Medapuram, P. Investigation of the universal behavior in symmetric diblock copolymer melts. Ph.D. thesis, University of Minnesota, 2015.

(151) Willis, J. D.; Beardsley, T. M.; Matsen, M. W. Simple and Accurate Calibration of the Flory–Huggins Interaction Parameter. *Macromolecules* **2020**, *53*, 9973–9982.

(152) Wilson, C. G.; Thomas, D. K.; Spooner, F. J. The crystal structure of Zr_4Al_3. *Acta Crystallogr.* **1960**, *13*, 56–57.

(153) Shoemaker, D. P.; Shoemaker, C. B. Concerning the relative numbers of atomic coordination types in tetrahedrally close packed metal structures. *Acta Crystallogr. Sect. B* **1986**, *42*, 3–11.

(154) Reddy, A.; Grason, G. M. A cornerstone of complex crystals. *Nat. Chem.* **2019**, *11*, 865–867.

(155) Ghasimakbari, T.; Morse, D. C. Order-Disorder Transitions and Free Energies in Asymmetric Diblock Copolymers. *Macromolecules* **2020**, *53*, 7399–7409.

(156) Matsen, M. W.; Bates, F. S. Block copolymer microstructures in the intermediate-segregation regime. *J. Chem. Phys.* **1997**, *106*, 2436–2448.

(157) Kim, S. A.; Jeong, K. J.; Yethiraj, A.; Mahanthappa, M. K.; Jeong, J.; Yethiraj, A.; Mahanthappa, M. K. Low-symmetry sphere packings of simple surfactant micelles induced by ionic sphericity. *Proc. Natl. Acad. Sci. USA* **2017**, *114*, 4072–4077.

(158) Li, C.; Dong, Q.; Li, W. Largely Tunable Asymmetry of Phase Diagrams of $A(AB)_n$ Miktoarm Star Copolymer. *Macromolecules* **2020**, *53*, 10907–10917.

(159) Qiang, Y.; Li, W.; Shi, A.-C. Stabilizing Phases of Block Copolymers with Gigantic Spheres via Designed Chain Architectures. *ACS Macro Lett.* **2020**, *9*, 668–673.

(160) Grzetic, D. J.; Delaney, K. T.; Fredrickson, G. H. Electrostatic Manipulation of Phase Behavior in Immiscible Charged Polymer Blends. *Macromolecules* **2021**, *54*, 2604–2616.

(161) Matsen, M. W. Self-consistent field theory for melts of low-molecular-weight diblock copolymer. *Macromolecules* **2012**, *45*, 8502–8509.

(162) Jiang, Y.; Zhang, X.; Miao, B.; Yan, D.; Chen, J. Z. Y. Microphase separation of short wormlike diblock copolymers with a finite interaction range. *Soft Matter* **2016**, *12*, 2481–2490.

(163) Park, S. J.; Yong, D.; Kim, Y.; Kim, J. U. Numerical implementation of pseudo-spectral method in self-consistent mean-field theory for discrete polymer chains. *J. Chem. Phys.* **2019**, *150*, 234901.

(164) Lai, C. T.; Shi, A.-C. Comment on "Quantifying the contribution of chain length heterogeneity on block copolymer self-assembly". *Giant* **2021**, *5*, 100046.

(165) Lifshitz, R. Explaining complex metals with polymers. *Proc. Natl. Acad. Sci. USA* **2014**, *111*, 17698–17699.

(166) Momma, K.; Izumi, F. VESTA 3 for three-dimensional visualization of crystal, volumetric and morphology data. *J. Appl. Crystallogr.* **2011**, *44*, 1272–1276.

(167) Suh, I. H.; Park, Y. S.; Kim, J. G. ORTHON: Transformation from triclinic axes and atomic coordinates to orthonormal ones. *J. Appl. Crystallogr.* **2000**, *33*, 994.

(168) Nima Moshtagh (2021). Minimum Volume Enclosing Ellipsoid (https://www.mathworks.com/matlabcentral/fileexchange/9542-minimum-volume-enclosing-ellipsoid), MATLAB Central File Exchange. Retrieved June 17, 2021.

(169) Ali Ozgul (2021). Homogen Integrate on Triangular Area and Tetrahedral Volume (https://www.mathworks.com/matlabcentral/fileexchange/13767-homogen-integrate-on-triangular-area-and-tetrahedral-volume), MATLAB Central File Exchange. Retrieved June 17, 2021.

Graphical TOC Entry